

RESEARCH OUTPUTS / RÉSULTATS DE RECHERCHE

Guest exchange in a biomimetic Zn^{II} cavity-complex

Nyssen, N.; Giraud, N.; Wouters, J.; Jabin, I.; Leherte, L.; Reinaud, O.

Published in:
Inorganic Chemistry Frontiers

DOI:
[10.1039/d3qi01271a](https://doi.org/10.1039/d3qi01271a)

Publication date:
2023

Document Version
Peer reviewed version

[Link to publication](#)

Citation for pulished version (HARVARD):

Nyssen, N, Giraud, N, Wouters, J, Jabin, I, Leherte, L & Reinaud, O 2023, 'Guest exchange in a biomimetic Zn^{II} cavity-complex: kinetic control by a catalytic water, through pore selection, 2nd sphere assistance, and induced-fit processes', *Inorganic Chemistry Frontiers*, vol. 10, no. 19, pp. 5772-5781. <https://doi.org/10.1039/d3qi01271a>

General rights

Copyright and moral rights for the publications made accessible in the public portal are retained by the authors and/or other copyright owners and it is a condition of accessing publications that users recognise and abide by the legal requirements associated with these rights.

- Users may download and print one copy of any publication from the public portal for the purpose of private study or research.
- You may not further distribute the material or use it for any profit-making activity or commercial gain
- You may freely distribute the URL identifying the publication in the public portal ?

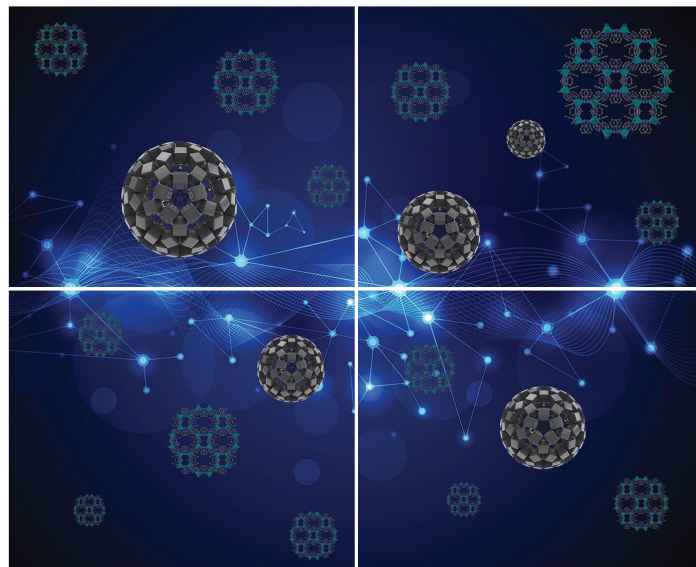
Take down policy

If you believe that this document breaches copyright please contact us providing details, and we will remove access to the work immediately and investigate your claim.

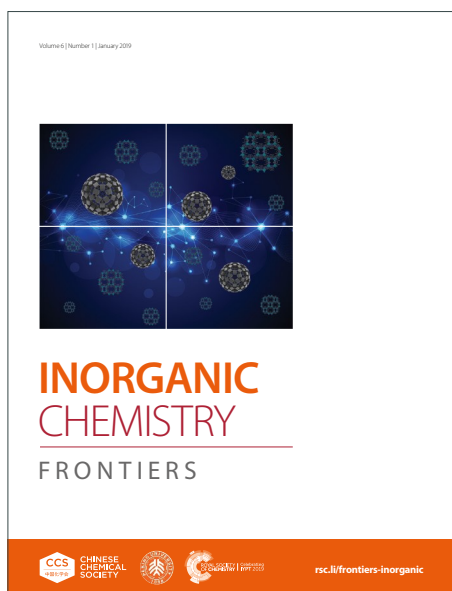
INORGANIC CHEMISTRY

FRONTIERS

Accepted Manuscript



This article can be cited before page numbers have been issued, to do this please use: N. Nyssen, N. Giraud, J. Wouters, I. Jabin, L. Leherte and O. Reinaud, *Inorg. Chem. Front.*, 2023, DOI: 10.1039/D3QI01271A.



This is an Accepted Manuscript, which has been through the Royal Society of Chemistry peer review process and has been accepted for publication.

Accepted Manuscripts are published online shortly after acceptance, before technical editing, formatting and proof reading. Using this free service, authors can make their results available to the community, in citable form, before we publish the edited article. We will replace this Accepted Manuscript with the edited and formatted Advance Article as soon as it is available.

You can find more information about Accepted Manuscripts in the [Information for Authors](#).

Please note that technical editing may introduce minor changes to the text and/or graphics, which may alter content. The journal's standard [Terms & Conditions](#) and the [Ethical guidelines](#) still apply. In no event shall the Royal Society of Chemistry be held responsible for any errors or omissions in this Accepted Manuscript or any consequences arising from the use of any information it contains.

Guest exchange in a biomimetic Zn^{II} cavity-complex: kinetic control by a catalytic water, through pore selection, 2nd sphere assistance, and induced-fit processes

Received 00th January 20xx,
Accepted 00th January 20xx

N. Nyssen,^{a,b} N. Giraud,^a J. Wouters,^c I. Jabin,^b L. Leherte,^{*c} O. Reinaud^{*a}

DOI: 10.1039/x0xx00000x

The kinetics of ligand exchange at a Zn^{II} center confined in a biomimetic environment is studied. The metal ion is bound to a TMPA unit covalently capping the calix[6]arene core. As such, the system is rigidified in a cone conformation open to the solvent at the large rim. At the small rim, the methyl groups of the anisole units lead to steric crowding, thus defining a small pore leading to the metal center. The exchange of an organic guest ligand (MeCN) for another (EtCN) is studied by ¹H NMR spectroscopy. It is shown that it is very slow under dry conditions (several hours at mM concentrations), but much faster in the presence of appreciable amounts of water. Kinetic analyses indicate that the exchange process involves the transient formation of an aqua complex that was independently synthesized and well characterized. Computer studies suggest that transient water coordination first occurs through the small rim pore, in *exo*-position. The water molecule then flips in *endo*-position, as the MeCN guest decoordinates and exits from the cavity through the large rim. This allows another organic guest ligand to get in, with release of the catalytic water to the solvent. Steered Molecular Dynamics simulations also show the assistance of the second coordination sphere of the metal ion for the *exo/endo* flipping process of the water ligand through H-bonding to the oxygenated small rim of the calixarene macrocycle. Importantly, it appeared that only water can play such a catalytic role, due to size selection by the pores defined by the calixarene small rim. From a biological point of view, it further substantiates the importance of water molecules and micro-environment on metal ion lability.

Introduction

Zn^{II} coordination in biology is important, displaying structural (eg. Zn fingers) or functional roles (Zn enzymes).¹⁻³ In these biological structures, Zn^{II} is coordinated to 3 or 4 amino-acid residues. In enzymes, an extra site is generally occupied by a water molecule that is the reactant (in hydrolases) or that is displaced by the reactant (e.g. a phosphate derivative as in alkaline phosphatases⁴ or an alcohol in alcohol dehydrogenase⁵). For all these enzymes, ligand exchange at the metal center is a key step in the catalysis. Ligand exchange is also a key factor that determines the stability of a structural site (inertness), or the Zn homeostasis. These exchange processes are difficult to study within the biological systems. Therefore, small model complexes are currently elaborated and studied to get specific insights into mechanisms at the molecular level.

Poly-aza tripods are classically used to mimic the poly-histidine rich biological sites found in metallo-enzymes. One of them, namely TMPA (*Tris*(2-PyridylMethyl)Amine), has been long studied for Fe and Cu biomimetic complexes. Less has been reported with Zn. While few examples of TMPA Zn complexes exist in literature, the main area of focus has been the utilization of Zn^{II} complexes in the cleavage of phosphodiester bonds. In those catalytic transformations, the kinetically active form was determined to be the corresponding Zn-aqua complex.⁶ The introduction of hydrogen bond donors has been shown to decrease the pKa of the bound water molecule and enhance the activity of such complexes, while also favoring the binding of phosphates ions.^{7,8} Indeed, it has long been recognized that the microenvironment around metal ions is a major factor that controls the reactivity/stability of Zn centers. One way to explore the supramolecular aspects relative to this microenvironment is to construct a well-defined and tunable microstructure around the metal ion labile site and evaluate the impact on its properties.⁹ Such a strategy allows to control the second coordination sphere of the metal ion, but also cavity effects related to ligand exchange. Being open to the solvent, the cavity acts not only as a receptor pocket, but also as a pore that will allow or not exogenous molecules to reach the metal center, thereby controlling its reactivity.

Ligands based on the calix[6]arene macrocycle connected to a tripodal nitrogenous core at the small rim are good mimics of the histidine-rich protein cavity.^{10,11} One of them, namely calix[6]TMPA (**L**, Scheme 1), presents a structure that is highly congested although open to the solvent. The calix[6]arene

^a Laboratoire de Chimie et de Biochimie Pharmacologiques et Toxicologiques, CNRS UMR 8601 Université Paris Cité, 45 Rue des Saints Pères, 75006 Paris, France, E-mail: Olivia.Reinaud@parisdescartes.fr

^b Laboratoire de Chimie Organique, Université libre de Bruxelles (ULB), Avenue F. D. Roosevelt 50, CP160/06, B 1050 Brussels, Belgium

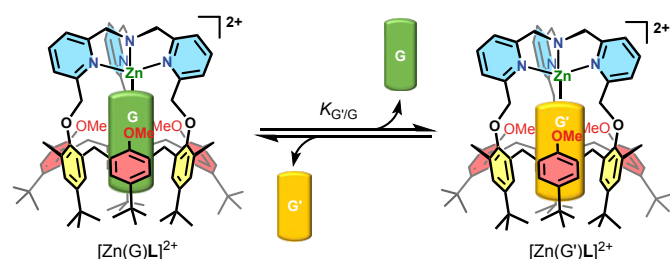
^c Laboratory of Structural Biological Chemistry, Unit of Theoretical and Structural Physical Chemistry, Department of Chemistry, NAMur Research Institute for Life Sciences (NARILIS), Namur Institute of Structured Matter (NISM), NAMur MEDicine & Drug Innovation Center (NAMEDIC), University of Namur, Rue de Bruxelles 61, B-5000 Namur, Belgium

† Electronic Supplementary Information (ESI) available: synthetic and procedure and characterization of [Zn(H₂O)L](ClO₄)₂, thermodynamic and kinetic measurements of guest exchanges through NMR spectroscopy, computational details. See DOI: 10.1039/x0xx00000x



macrocycle is *tris*-methylated on alternate position of the phenol units, and covalently capped by a TMPA unit through short methylene linkers to the three other phenol units. As such, access to the metal ion bound in the TMPA cap through the small rim pores is highly restricted by steric congestion between the methoxy substituents and the cap methylene linkers.

In a recent study,¹² we reported the synthesis of the corresponding Zn^{II} acetonitrile complex that is 5-coordinate with a guest acetonitrile molecule bound in the calixarene cavity. A thermodynamic study of ligand exchanges monitored by NMR spectroscopy showed that the macrocyclic structure is rigidified in a cone conformation. However, it keeps some flexibility as the three anisole “walls” can rotate along the calix methylene groups for a few degrees, as a function of the size of the included guest ligand. Along our studies, we noticed some surprisingly slow processes: first, coordination of the Zn^{II} dication required heating for hours; second, the exchange of the MeCN guest for EtCN took several hours to reach equilibrium under some experimental conditions. These observations stand in strong contrast with the behavior of simple TMPA metal complexes, devoid of cavity, for which metalation and ligand exchange proceed almost instantaneously. Wanting to know more about these phenomena, we undertook a detailed study relative to the kinetics of exchange between two representative organic guest ligands (G and G', Scheme 1), namely MeCN and EtCN, which is the subject of the present article.



Scheme 1. Guest exchange G/G' equilibrium inside the cavity of [Zn(G)L]²⁺.

Results

Characterization of the aqua complex

Complex [Zn(MeCN)L](ClO₄)₂ was synthesized as previously reported, by reacting the calixarene ligand L with a stoichiometric amount of the Zn^{II} perchlorate salt in MeCN. Noticeably, the complexation process required heating the solution for several hours. Indeed, protonation of L occurs immediately in solution in a first step and complexation necessitates the displacement of the proton by the metal ion in a second slow, but thermodynamically favored, step.¹² The dicationic complex was isolated as the acetonitrile complex and characterized by ¹H NMR spectroscopy. The overall signature attested to a C_{3v} symmetry with the Zn^{II} center bound to the TMPA cap and one molecule of acetonitrile sitting inside the calixarene cavity as attested by its high field δ shift (-0.62 ppm).

We noticed however that, when dissolved in wet acetone, a second species was present. The latter did not correspond to the protonated ligand and vanished upon addition of small amounts of MeCN. Suspecting that it could correspond to the aqua complex, we repeated the complexation process with a 1:1 mixture of ligand L and Zn^{II} salt in a non(/poorly)-coordinating solvent, namely acetone. The complexation also required heating the solution for several hours. The isolated complex was characterized by various spectroscopies. The IR spectrum confirmed the presence of two perchlorates as counterions (see the SI). The ¹H NMR spectrum (Figure 1 Bottom-blue) is typical of a C_{3v} symmetrical structure with a cone conformation for the calix[6]arene macrocycle. As for the nitrile complex, the pyridyl protons are low field shifted compared to the free ligand, thus attesting to the coordination of the Lewis acidic metal ion Zn^{II}. The two sets of aromatic H_{Ar} and *t*Bu protons display closer δ shifts for the aqua complex ($\Delta\delta \sim 0.2$ ppm) than for the MeCN complex (~ 0.7 ppm). This suggests an average straighter conformation for the calixarene host, consistently with the smaller size of the guest water molecule. The coordinated water molecule could be identified under relatively dry conditions, through two signals at 8.28 and 8.46 ppm, each one integrating for one proton. These two signals vanished upon D₂O addition. Saturation transfer experiments with free water and NOESY measurements further confirmed their attribution (see the SI). These low-field shifted δ values indicate that the water molecule is bound to the Lewis acidic Zn^{II} center and sits at the level of the small rim of the calixarene structure, away from the anisotropic cone of the aromatic walls. It is noteworthy that each proton of the coordinated water molecule is differentiated from the other. This reflexes strong electrostatic interaction with the oxygen atoms belonging to the calixarene small rim that slows down the rotation of the water molecule inside the structure. The differentiation of the two protons can be due to a stronger interaction of one of the water protons with a calixarene oxygen atom. Addition of an aliquot of MeCN to this aqua complex led to the appearance of a high-field peak at -0.62 ppm corresponding to the MeCN ligand included in the cavity (Figure 1 Top-purple), thus attesting to the formation of the MeCN complex. The exchange was slow at the ¹H NMR shift time scale, but fast at the experimental time scale. A careful titration of the aqua complex by acetonitrile (see the SI) confirmed that one water molecule is coordinated to the Zn^{II} ion, and no extra water guest is present, either in the cavity or in *exo*-position.

Kinetic study of the acetonitrile/propionitrile exchange

The exchange between two nitriles was followed by ¹H NMR spectroscopy by recording multiple spectra over the course of several hours of a solution of one nitrile complex in presence of a known amount of the other nitrile in deuterated acetone. A representative example is shown in Figure 2. The amount of each complex was calculated by integrating the two signatures in slow exchange on the NMR shift time scale (SI). However, we noticed that the rate of exchange varied not only with the



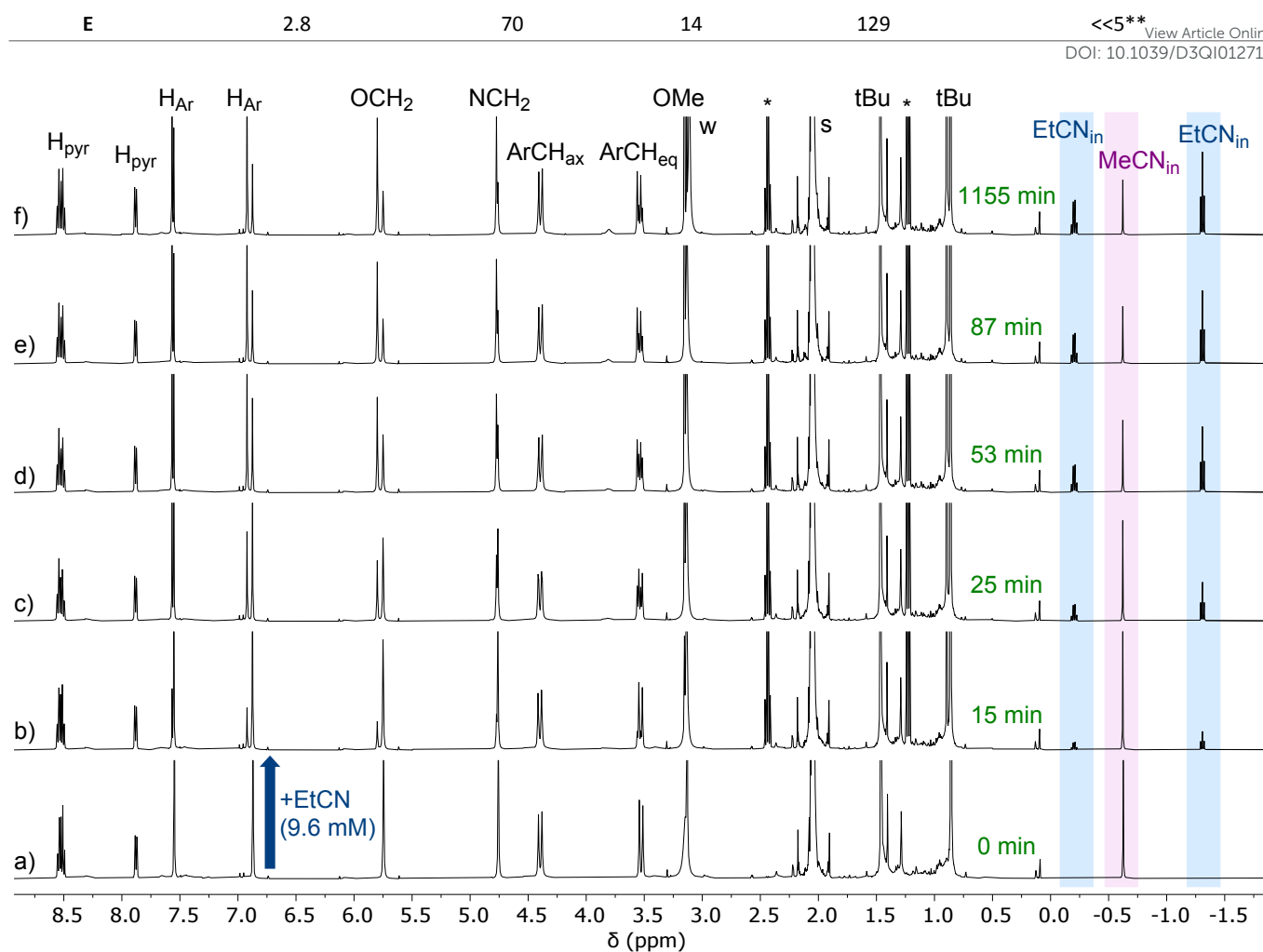


Figure 2. ^1H NMR spectra (300 K, 500 MHz, acetone- d_6) recorded during the titration of $G = \text{MeCN}$ by $G' = \text{EtCN}$. Initial conditions in a) $[\text{Zn}(\text{MeCN})\text{L}]^{2+} = 3.7 \text{ mM}$, $[\text{free MeCN}] = 92 \text{ mM}$, $[\text{EtCN}] = 0 \text{ mM}$, $[\text{H}_2\text{O}] = 20 \text{ mM}$. Percentage of EtCN complex in solution: a) 0%, b) 17%, c) 38%, d) 41%, e) 59%, f) 71%. This experiment is reported as entry A in Table 1. Full conversion corresponds to the amount of EtCN complex formed at equilibrium under these experimental (71%). The “t(50% conversion)” is then the time at which we have 35.5% of EtCN complex in solution. *: free EtCN.

Setting that $x = [\text{MeCN}_{\text{in}}]$ and $c = [\text{total calixarene}]$, we obtain:

$$-\frac{dx}{dt} = k_2 K_1 [w_0] \frac{([\text{EtCN}_0] - c + x)x}{[\text{MeCN}_0] - x} \quad (\text{Eq. 2})$$

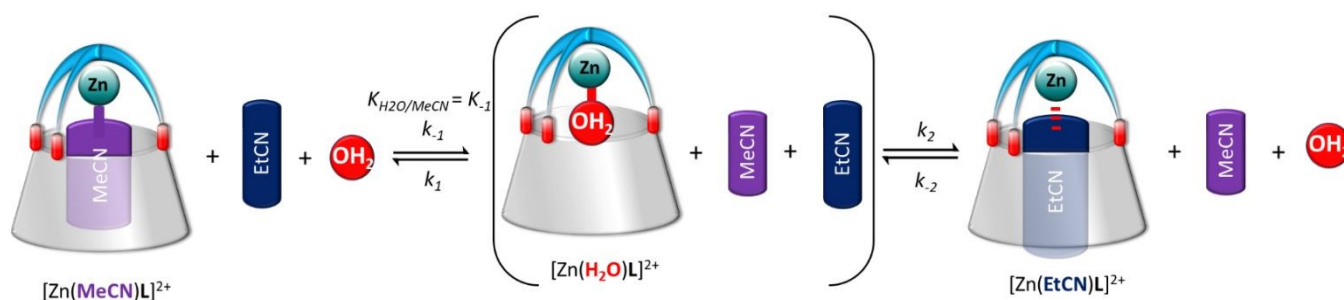
And thus:

$$-\frac{1}{\frac{([\text{EtCN}_0] - c + x)x}{K_1 [\text{MeCN}_0] - x}} dx = k_2 [w_0] dt \quad (\text{Eq. 3})$$

which gives, after integration:

$$F(x) = \frac{[\text{MeCN}_0] \text{Ln}(x) - ([\text{EtCN}_0] + [\text{MeCN}_0] - c) \text{Ln}([\text{EtCN}_0] - c + x)}{K_1([\text{EtCN}_0] - c)} = -k_2 [w_0] t \quad (\text{Eq. 4})$$

(the subscript “0” defines “total amount of”; $[w_{\text{out}}] \approx [w_0]$, “in” and “out” refer to the calixarene cavity)



Scheme 2. Proposed pathway for the guest exchange involving the transient formation of the aqua complex.



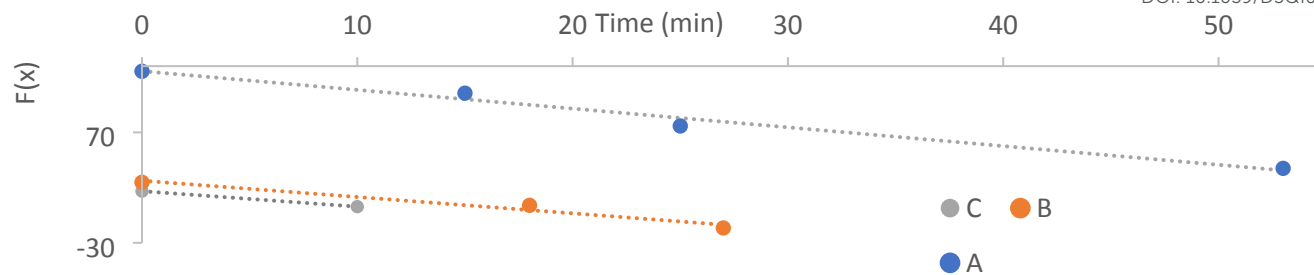
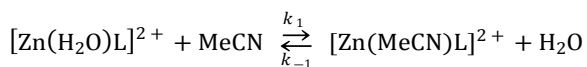


Figure 3. Kinetic fit of the ^1H NMR analyses. For the expression of $F(x)$, see (Eq. 4). A,B,C refers to experiments of Table 1.

Figure 3 shows full agreement with the working hypothesis as the data recorded for the 3 different experiments show a linear relationship in agreement with Equation (4). The exchange kinetic constant is thus: $k_2 = 0.090 \pm 0.004 \text{ mM}^{-2}\text{min}^{-1}$. From this value, we can deduce that $k_2 = 0.015 \pm 0.002 \times 10^{-3} \text{ mM}^{-2}\text{min}^{-1}$.

NOESY measurement

As the MeCN/ H_2O exchange process is much faster than that of MeCN/EtCN, we have chosen to monitor it by NMR using EXchange Spectroscopy (EXSY). For this purpose, a solution containing a mixture of the MeCN and aqua complexes was prepared, and we have recorded a ^1H - ^1H 2D NMR NOESY spectrum on this sample. On the resulting data, we clearly observe several sets of correlations for the complex, revealing a slow exchange on the NMR shifts time scale between the MeCN and the aqua form. Figure 4 shows the region of the resulting 2D spectrum where this correlation pattern is observed. We have thus recorded a series of EXSY spectra, varying the mixing time to monitor this slow exchange process (a representative 2D map acquired at 600 MHz is described in the SI). The volume of the resolved correlation patterns was measured for each mixing time value. The resulting build-up curves that were obtained for the selected diagonal and cross peaks arising from the exchange process between the aqua and MeCN complexes can be modelled using modified Bloch equations accounting for proton longitudinal relaxation and the formal equilibrium:



The analysis of the NOESY correlations involving (i) an aromatic proton from the calixarene ligand, and (ii) the methyl protons from MeCN, both undergoing a chemical exchange between the aqua and MeCN complexes, yielded k_1 values from 2.2 to $11 \text{ min}^{-1}\text{mM}^{-2}$ and $k_{-1} = 0.02 \pm 0.02 \text{ min}^{-1}\text{mM}^{-2}$. This result yields a calculated value for $K_{\text{MeCN}/\text{H}_2\text{O}} = k_1/k_{-1} = 110$ to 500, in good agreement with the value of 200 measured by titration (see above and Scheme 2). These kinetic data, when compared to those measured for the EtCN/ H_2O exchange ($k_2 = 0.090 \text{ mM}^{-2}\text{min}^{-1}$ and $k_2 = 0.015 \times 10^{-3} \text{ mM}^{-2}\text{min}^{-1}$), indicate that both, entrance and exit of the nitrilo guest are three orders of magnitude faster for MeCN than for EtCN. Hence, the rates are obviously related to the size of the guest. This corresponds to the energy cost to open the small rim door constituted by the 3 *t*Bu substituents of the most rigid aromatic units, namely those

connected to the TMPA cap. Such a kinetic differentiation is reminiscent of a previous study reported for a Cu^{I} complex obtained with a calix[6]arene functionalized by three α -methylpyridyl groups. Indeed, it was shown that part of the activation energy for the exit of the acetonitrile guest stems from the *t*Bu door into which the guest “bump” during the dissociative process.¹³

In order to clarify the role of the water molecule and the reason for which the aqua-complex is involved as a necessary intermediate for the exchange between two nitrile guests, we have carried out molecular computing studies. The idea was to start with the acetonitrile complex and identify the pathway through which the water molecule becomes in interaction with the Zn^{II} center, whereas the MeCN guest leaves the cavity.

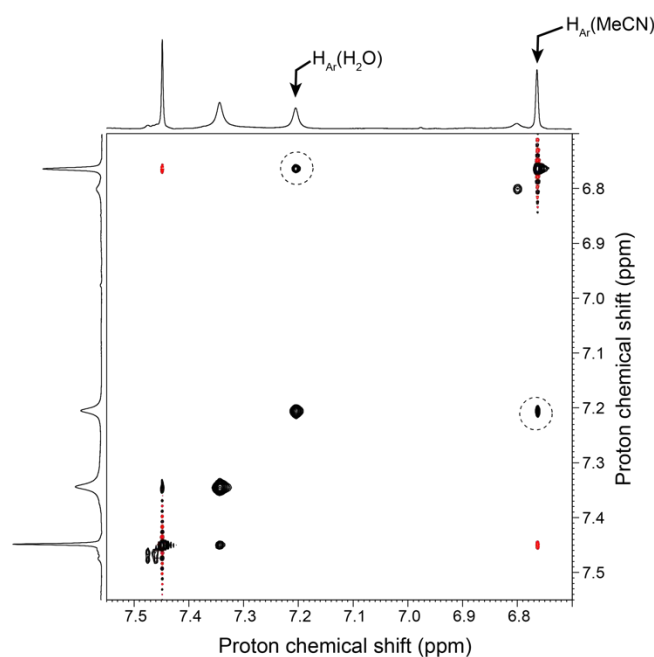


Figure 4. Selected region of a 2D ^1H - ^1H NOESY spectrum (500 MHz) of a solution containing a mixture of the aqua and MeCN Zn complex in acetone- d_6 . This spectrum was recorded with a mixing time of 1.5 s. The sample was prepared with 0.9 eq. of MeCN and 200 eq. of H_2O . Correlations reflecting the exchange process between MeCN and H_2O in the cavity of the Zn complex are highlighted with a dotted circle. Other regions of interest of this 2D map are shown together with the 1D ^1H NMR spectrum in Supplementary Information.



Steered Molecular Dynamics simulation of the guest-water exchange

To favor the guest-water exchange in the calixarene structure, Molecular Dynamics (MD) and Steered MD (SMD) simulations of a calixarene-MeCN complex interacting with a water molecule were carried out in vacuum at 300 K using the program GROMACS2020,¹⁴ as detailed in the SI. Water and the small molecules were modeled using the TIP3P and CHARMM27 force fields, respectively. The simulations were carried out with four atom position restraints placed on the *N* atoms of the calixarene cap, while restraining the four Zn-N_{cap} distances to avoid exaggerated displacement of the Zn²⁺ ion during the approach and the insertion of water inside the calixarene cavity. The system was first optimized using a steepest descent algorithm (Figure 5, structure **A**). Then, the MD total equilibration stage duration was set to 2,100 ps. At the end of this stage, the water molecule more closely interacts with Zn^{II} (Figure 5, structure **B**). Afterwards, the SMD stage was carried out for a period of 60 ps. A pulling force was applied to the center of mass of MeCN to progressively evacuate MeCN from the calixarene cavity. As illustrated in the SI, the time-dependence of the water interaction energy with its neighborhood allows to model the substitution of MeCN as a stepwise process.

Step 1: Coordination of water

At the end of the preliminary optimization stage, the total intermolecular interaction energy (IIE) value of the molecule of water (defined as the sum of IIEs with the calixarene, Zn, and MeCN) is equal to -40 kJ mol⁻¹. Starting from the optimized structure (Figure 5, structure **A**), the water molecule evolves around the calixarene until it reaches a stabilized position facing the Zn²⁺ ion, at 1,701.0 ps (Figure 5, structure **B**). It is hydrogen-bonded to an O_{methoxy} atom of the calixarene structure (see the SI) and a deformation of the calixarene cap is observed. The interaction energy value drastically decreases from a value of -54 kJ mol⁻¹ at t = 1,700.0 ps to a value of -142 kJ mol⁻¹ at t = 1,701.0 ps, and the O_{water}-Zn distance is reduced to a value of about 2 Å (see the SI). This gives rise to a stable 6-coordinate intermediate presenting a pseudo-octahedral environment due to the simultaneous coordination of water and MeCN. Such an intermediate is observed until the end of the equilibration stage, i.e., t = 2,100.0 ps.

Step 2: Substitution of MeCN by water

Snapshots at various times during the insertion procedure (60 ps) are displayed in Figure 5 (structures **I1** to **I4**). When the pulling force is applied to the MeCN ligand, the substitution of MeCN by H₂O does not immediately take place. Indeed, the water molecule position and orientation remain stable during 29.7 ps. H₂O closely approaches the calixarene cavity after 29.8 ps of the pulling stage (Figure 5, structure **I1**). At that moment, the water molecule is hydrogen-bonded to a methoxy group of the calixarene structure (Figure 5 inset, and SI) and its second H atom is oriented towards the N_{MeCN} atom at a distance of 1.91

Å. Also, the water interaction energy value has decreased to a value of -173 kJ mol⁻¹. The O_{water}-Zn distance remains slightly larger than 2 Å (SI), while the N_{MeCN}-Zn distance begins to increase (SI). Shortly after, at t = 29.9 ps when MeCN is farther from Zn, the water molecule begins its insertion into the calixarene (Figure 5, structure **I2**). Its interaction energy value is -192 kJ mol⁻¹. At t = 30.0 ps (Figure 5, structure **I3**), the water interaction energy reaches a value of -231 kJ mol⁻¹.

Step 3: Relaxation of the calixarene 3D structure

Starting from the coordination step (Step #1), H₂O remains hydrogen-bonded to the calixarene structure (Figure 5 inset, and SI). At t = 30.0 ps, the deformation of the calixarene cap observed at step #1 is still visible, but the C₃ symmetry is recovered at around 42.0 ps (see the SI). Then, due to the folding of a *t*Bu group inside the calixarene, the C₃ symmetry is preserved only at the level of calixarene cap, as illustrated at t = 60.0 ps of the SMD trajectory (Figure 5, structure **I4** and SI) where the two shortest H_{water}-O_{methoxy} distances are equal to 2.64 and 2.94 Å. A slight relaxation is observed in the mean Zn-N_{calix} distance profile with an overall decrease of 0.003 nm (see the SI) and no large energy changes are observed. At that moment, the water interaction energy value is equal to -236 kJ mol⁻¹. Hence, after substitution of MeCN by H₂O around 43 ps of the SMD trajectory, the calixarene structure undergoes a folding of one *t*Bu group towards the calixarene cavity, which coincides with a decrease in the H₂O and *t*Bu interaction energy values (SI and Figure 5 inset, respectively). To confirm the likelihood of such a fold, the structure **I4** was submitted to an optimization stage at the MP7 semi-empirical level using the program MOPAC¹⁵ which corroborates the SMD results, in agreement with the NMR observations (Figure 5, structure **C**). Particularly, in the final optimized structure, the water molecule reorients to form a H-bond with one of the calixarene methoxy groups. Such a self-inclusion process of a *t*Bu substituent in the cavity was previously observed by ¹H NMR spectroscopy at low T with a closely related calix[6]arene-based Cu^I funnel complex binding carbon monoxide.¹⁶ With this small guest ligand, a “3-step valve” was evidenced between three *t*Bu substituents going alternatively in *in* and *out* positions. When fast at the NMR shift time scale (*ie.* at RT), this led to a pseudo C_{3v} signature with an apparent straight conformation, exactly as observed here for the aqua-complex.

To support the observation, the 60 ps long SMD simulation was continued by a 4,000 ps conventional MD run using initial random atom velocities. Unfolding-refolding events were observed with exchange between the *t*Bu moieties until t = 1576.3 ps (see the SI). Then, *t*Bu exchange stops and the last folded conformation remains present until the end of the simulation. In this structure, a strong H-bond connects regularly one of the hydrogen atoms of the water guest to an anisole unit during 4 % of the time, a percentage equally shared by both H atoms of the water molecule.

The computer simulations were also conducted with acetone as a solvent instead of vacuum and similar results were obtained (see the SI). The water molecule first gets close to the calixarene



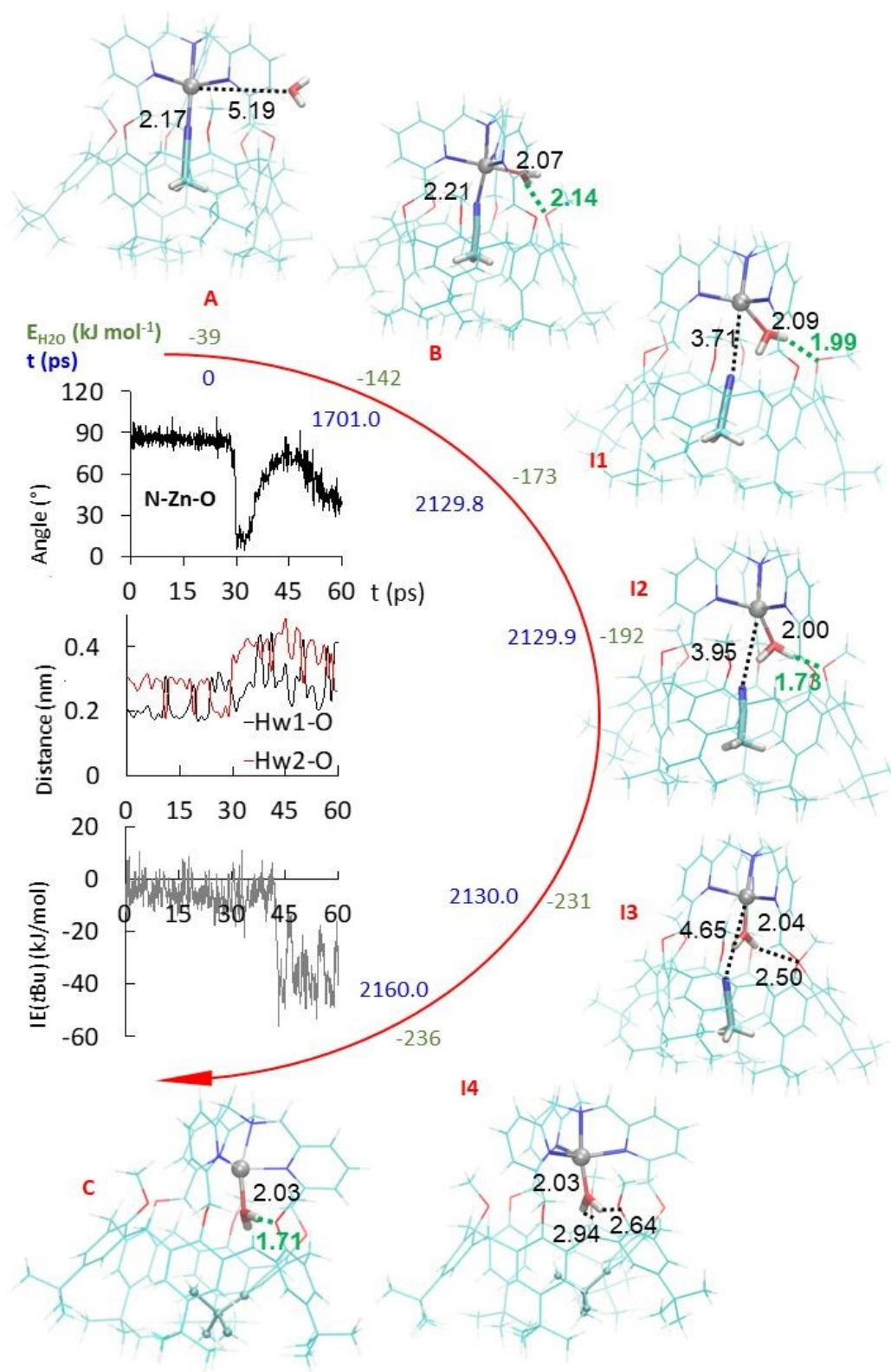


Figure 5. Stepwise substitution of MeCN guest by a water molecule following an associative pathway, as obtained from the 2,160 ps MD and SMD trajectories in vacuum at 300 K. Initial optimized structure - A, snapshot at 1,701 ps of the MD trajectory (coordination of H₂O - B), at $t = 29.8$ of the SMD trajectory (insertion stage - I1), 29.9 ps (insertion stage - I2), 30.0 ps (insertion stage - I3), and 60.0 ps (final structure - I4). Semi-empirical MP7 optimized structure (C). Dotted lines refer to selected interatomic distances (in Å). Green dotted lines depict hydrogen bonds. The folded tBu moiety is displayed using ball and stick representations in I4 and C. Inset from top to bottom (obtained from the 60 ps long SMD trajectory): Variation of the NMeCN- Zn^{II}-Owater angle and Hwater...OME distances; tBu-calixarene short-range interaction energy profile.



structure and deforms it while it coordinates Zn^{II}. In the solvated case however, H₂O is first hydrogen bonded to two acetone molecules. Then, similarly to the vacuum case, it forms a hydrogen bond with a methoxy group of the calixarene. The simulations were also performed with EtCN as an initial guest instead of MeCN, and same results were obtained for the substitution process. Finally, when the water molecule initially out of the cavity is replaced by MeCN, close interaction with the Zn center in *exo*-position was observed but at a distance that is much too long to correspond to a coordination bond. Consistently, the interaction energy of the *exo*-MeCN molecule is not significantly reduced compared to other positions. It remains very mobile and, after a while, tends to be trapped at the level of the cap of the calixarene. Similar results were obtained with MeOH replacing H₂O (see the SI). Coordination of the MeCN and MeOH molecules by Zn^{II} are then triggered by removing the *endo*-ligand MeCN during the whole MD simulations. It likely favors the strong deformation of the calixarene structure, but it does not initiate the insertion of the molecule that stays outside the calixarene cavity. Nevertheless, the insertion of MeOH can be artificially produced by the application of a steering force to pull the ligand inside the calixarene through the small rim. Such a SMD simulation was carried out using the same methodology as used for pulling the *endo*-ligand outside the cavity. Interestingly, MeCN does not enter the calixarene using that approach. Hence, water is the only ligand to spontaneously enter the calixarene cavity through the small rim: it is small enough to flip from the *exo*-position to the *endo*-position through the small pore existing at the calixarene small rim, whereas MeCN and MeOH appear to be either too large or not energetically stabilized at the level of the small pore. This suggests that the only (or most probable) pathway for an organic ligand to coordinate the metal center in *endo*-position, inside the cavity, is to go *through* the large rim of the calix-funnel. This inclusion process is, likely for a steric reason, impossible when the cavity is already occupied by an organic guest, whereas a water guest can get in from the small rim.

In summary, the simulations show that the preliminary step for a ligand to enter the cavity through the calixarene small rim is to be immobilized strongly enough, through a coordination bond to the metal center to the calixarene structure. Without such binding, the ligand remains free to move around the calixarene structure. Then, if the *exo*-ligand is small enough, it can flip into the cavity when the guest ligand leaves, thereby avoiding the formation of an "empty cavity" intermediate during guest exchange. Hence, water seems very unique as it can bind to Zn^{II} in *exo*-position and flip into the cavity in *endo*-position, thus allowing the guest-Zn bond cleavage and the exit of the guest, and conversely. Quite interestingly, and subtly, the

key flipping process involves transient assistance of an oxygen atom present at the small rim of the calixarene acting as H-bond acceptor in the second coordination sphere of the metal ion.

Discussion

It may appear surprising that a simple dissociative mechanism for guest-exchange is not at work in this system. Indeed, direct displacement of the guest would leave a 4-coordinate intermediate, which should not be so unstable. One explanation could rely on the rigidity of the system. Indeed, the capping TMPA unit of ligand **L** constrains the calixarene macrocycle in a cone conformation with aromatic units lying alternatively in in/out position relative to the cavity. This alternate cone conformation is the opposite to the one adopted by the more flexible ligands: three imidazole arms¹⁷ or a TREN (Tris(2-aminoethyl)amine) unit¹⁸. The relatively straight conformation adopted by calixarene **L** is explained by the fact that the aromatic units connected to the cap are obliged to sit in a position that projects their oxygen atom toward the outside (Figure 6). Consequently, the three other aromatic units, bearing methoxy groups, are constrained to orient their oxygen atom toward the inside. This creates a high steric hindrance that defines the pore for *exo*-binding and allows 2nd sphere assistance for water *exo*-binding and *endo*-flipping. Importantly also, the rigidified calix core of Zn^{II}**L** restricts the induced-fit process observed with the other systems that can adopt a flattened conformation, thus shrinking the cavity space in the absence of guest. As a result, the energy cost for leaving a fully empty cavity is probably much higher with **L**; it explains the fact that the water ligand flips into the cavity whereas the guest leaves. The resulting new 5-coordinate intermediate then undergoes partial insertion of one of its *t*Bu substituent present at the large rim in order to optimize the cavity filling. This leads to a fully stable aqua complex that could be independently synthesized and fully characterized.

Finally, it is worth noting that the *t*Bu group that is partially included in the cavity space of the aqua complex constitutes a gate that needs to be open for guest leaving and guest entering. These in/out phenomena may explain the impressive difference of rate exchange for the MeCN and EtCN guests in both directions. The corresponding difference in activation energies (ca. 3 orders of magnitude \sim 17 kJ/mol) may correspond to the interaction energy difference between the *t*Bu gate and the ethyl vs. methyl group of the guest during the leaving and entering processes. Interestingly, such an inertness under dry conditions was previously observed¹⁹ with the Cu complexes of the very same ligand **L** and it was shown that water guests regulate its redox activity.²⁰ In the present study, we evidence the role of water for ligand exchange, a role that was not elucidated before.

View Article Online
DOI: 10.1039/D3QI01291A



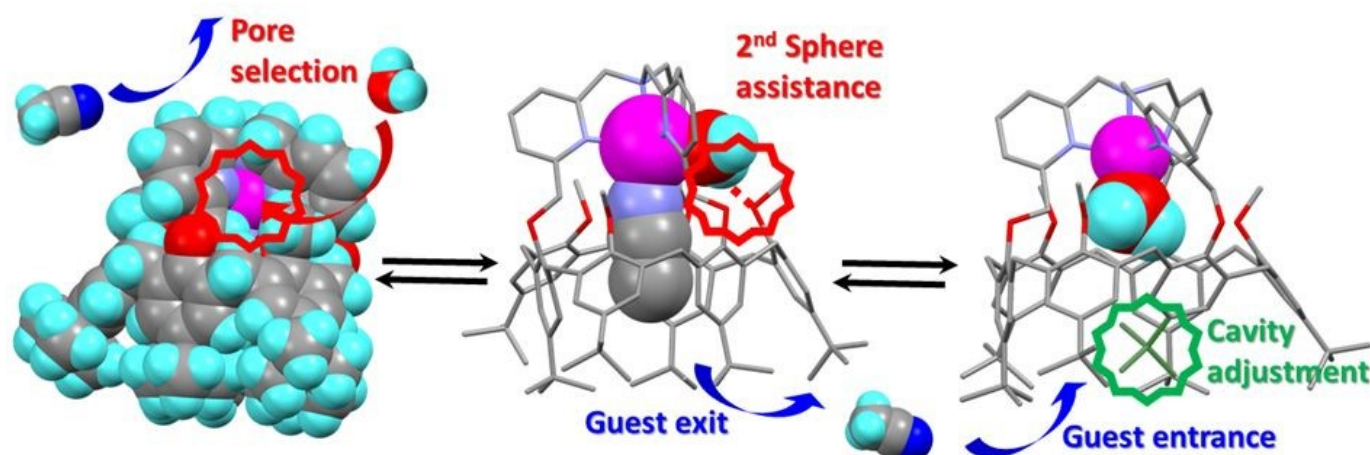


Figure 6. Key steps for the guest exchange catalyzed by a water molecule evidencing: (left) Pore-size selection for the exo-access to the metal center; (center) H-bonding assistance for the water ligand flipping from an exo to an endo position; (right) *t*Bu partial insertion for filling the cavity space.

Conclusion

In conclusion, we have described a very special system where the Zn^{II} cation is embedded in a nitrogenous cap connected to a cavity open to the solvent, for which guest ligand exchange is under the control of a single water molecule. The exchange process involves a first associative step where a water molecule binds the Zn center in *exo*-position, thus leading to an octahedral intermediate. The second step is the intramolecular substitution of the *endo*-bound guest (G) by the *exo*-bound water to give rise to a 5-coordinate aqua Zn complex with concomitant expulsion of the initial guest (G). In virtue of the micro-reversibility principle, the substitution of the *endo*-bound aqua ligand by a new organic guest (G') follows the same pathway, with entrance of the new guest (G') at the large rim, and expulsion of the water molecule by the side, at the small rim. Hence, the water molecule acts as a catalyst and is very unique in its catalytic role: it first binds to the metal center in an *exo*-position, and flips into the pore at the calixarene small rim with the assistance of an oxygen atom of the host structure acting as H-bond acceptor. Other studied molecules are too large or do not, under the selected calculation conditions, spontaneously initiate the insertion step through coordination to Zn^{II}, which is required before insertion under the current calculation conditions. As a spectacular result, G exchanges for G' is fast only in the presence of water, and water plays the role of a very unique catalyst that controls the kinetics of guest exchange at the metal center thanks to a pore selection and 2nd coordination sphere assistance.

All in all, this study represents the second case ever reported in the literature of well-characterized molecular metal complex for which ligand exchange is under the unique control of a single water molecule.¹⁷ Here, the control relies on pore selection, 2nd sphere assistance through transient H-bonding, and host-guest induced fit. From a biological point of view, it further substantiates the importance of water molecules on metal ion

stability, a property that is key for the stability of structural Zn sites in proteins, for Zn-enzyme activity, as well as for homeostasis

Conflicts of interest

There are no conflicts to declare.

Acknowledgements

NN thanks the « Ministère de l'Enseignement Supérieur et de la recherche » and « Université Paris Cité » and the CCCI funding from « Université libre de Bruxelles ».

LL and JW used resources of the 'Plateforme Technologique de Calcul Intensif (PTCI)' (<http://www.ptci.unamur.be>) located at the University of Namur, Belgium, which is supported by the FNRS-FRFC under the conventions No. 2.5020.11. The PTCI is member of the 'Consortium des Équipements de Calcul Intensif (CÉCI)' (<http://www.ceci-hpc.be>), funded by the 'Fonds de la Recherche Scientifique de Belgique (F.R.S.-FNRS)'.

Notes and references

1. W. N. Lipscomb and N. Sträter, Recent Advances in Zinc Enzymology, *Chemical Reviews*, 1996, **96**, 2375-2434.
2. W. Maret and Y. Li, Coordination Dynamics of Zinc in Proteins, *Chemical Reviews*, 2009, **109**, 4682-4707.
3. A. Krężel and W. Maret, The biological inorganic chemistry of zinc ions, *Archives of Biochemistry and Biophysics*, 2016, **611**, 3-19.
4. B. Stec, K. M. Holtz and E. R. Kantrowitz, A revised mechanism for the alkaline phosphatase reaction involving three metal ions¹¹ Edited by R. Huber, *Journal of Molecular Biology*, 2000, **299**, 1303-1311.
5. B. V. Plapp, B. R. Savarimuthu, D. J. Ferraro, J. K. Rubach, E. N. Brown and S. Ramaswamy, Horse Liver Alcohol



- Dehydrogenase: Zinc Coordination and Catalysis, *Biochemistry*, 2017, **56**, 3632-3646.
6. G. Feng, J. C. Mareque-Rivas, R. Torres Martín de Rosales and N. H. Williams, A Highly Reactive Mononuclear Zn(II) Complex for Phosphodiester Cleavage, *Journal of the American Chemical Society*, 2005, **127**, 13470-13471.
7. J. C. Mareque-Rivas, R. Prabakaran and R. T. Martín de Rosales, Relative importance of hydrogen bonding and coordinating groups in modulating the zinc–water acidity, *Chemical Communications*, **1**, 2004, 76-77
8. J. C. Mareque-Rivas, R. Torres Martín de Rosales and S. Parsons, The affinity of phosphates to zinc(ii) complexes can be increased with hydrogen bond donors, *Chemical Communications*, **5**, 2004, 610-611.
9. R. Gramage-Doria, D. Armspach and D. Matt, Metallated cavitands (calixarenes, resorcinarenes, cyclodextrins) with internal coordination sites, *Coordination Chemistry Reviews*, 2013, **257**, 776-816.
10. J.-N. Rebilly, B. Colasson, O. Bistri, D. Over and O. Reinaud, Biomimetic cavity-based metal complexes, *Chemical Society Reviews*, 2015, **44**, 467-489.
11. D. Coquière, S. Le Gac, U. Darbost, O. Sénèque, I. Jabin and O. Reinaud, Biomimetic and self-assembled calix[6]arene-based receptors for neutral molecules, *Organic & Biomolecular Chemistry*, 2009, **7**, 2485-2500.
12. P. Aoun, N. Nyssen, S. Richard, F. Zhurkin, I. Jabin, B. Colasson and O. Reinaud, Selective Metal-ion Complexation of a Biomimetic Calix[6]arene Funnel Cavity Functionalized with Phenol or Quinone, *Chemistry – A European Journal*, 2023, **29**, e202202934.
13. Y. Rondelez, A. Duprat and O. Reinaud, Calix[6]arene-Based Cuprous “Funnel Complexes”: A Mimic for the Substrate Access Channel to Metalloenzyme Active Sites, *Journal of the American Chemical Society*, 2002, **124**, 1334-1340.
14. M. J. Abraham, T. Murtola, R. Schulz, S. Páll, J. C. Smith, B. Hess and E. Lindahl, GROMACS: High performance molecular simulations through multi-level parallelism from laptops to supercomputers, *SoftwareX*, 2015, **1-2**, 19-25.
15. J. J. P. Stewart, Stewart Computational Chemistry, Colorado Springs, CO, USA (2016), [HTTP://OpenMOPAC.net](http://OpenMOPAC.net) (last accessed 20 Dec. 2022)
16. Y. Rondelez, O. Sénèque, M.-N. Rager, A. F. Duprat and O. Reinaud, Biomimetic Copper(I)–CO Complexes: A Structural and Dynamic Study of a Calix[6]arene-Based Supramolecular System, 2000, **6**, 4218-4226.
17. E. Brunetti, L. Marcelis, F. E. Zhurkin, M. Luhmer, I. Jabin, O. Reinaud and K. Bartik, A Water Molecule Triggers Guest Exchange at a Mono-Zinc Centre Confined in a Biomimetic Calixarene Pocket: a Model for Understanding Ligand Stability in Zn Proteins, *Chemistry – A European Journal*, 2021, **27**, 13730-13738.
18. U. Darbost, X. Zeng, M.-N. Rager, M. Giorgi, I. Jabin and O. Reinaud, X-ray and Solution Structures of the First Zn Funnel Complex Based on a Calix[6]aza-cryptand, 2004, **22**, 4371-4374.
19. N. Le Poul, B. Douziech, J. Zeitouny, G. Thiabaud, H. Colas, F. Conan, N. Cosquer, I. Jabin, C. Lagrost, P. Hapiot, O. Reinaud and Y. Le Mest, Mimicking the Protein Access Channel to a Metal Center: Effect of a Funnel Complex on Dissociative versus Associative Copper Redox Chemistry, *Journal of the American Chemical Society*, 2009, **131**, 17800-17807.
20. N. Le Poul, B. Colasson, G. Thiabaud, D. J. Dit Fouque, C. Iacobucci, A. Memboeuf, B. Douziech, J. Rezac, B. Prangé, A. d. I. Lande, O. Reinaud and Y. Le Mest, Gating the electron transfer at a monocopper centre through the supramolecular coordination of water molecules within a protein chamber mimic, *Chemical Science*, 2018, **9**, 8282-8290.



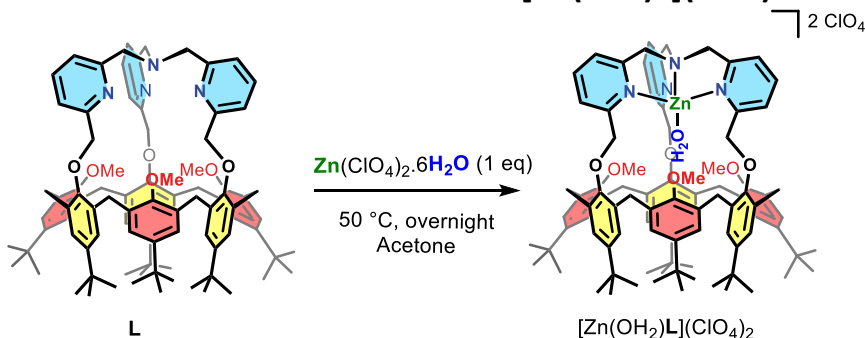
Supplementary Information

Guest exchange in a biomimetic Zn^{II} cavity-complex: kinetic control by a catalytic water, through pore selection, 2nd sphere assistance, and induced-fit processes

N. Nyssen,^{a,b} N. Giraud,^a J. Wouters,^c I. Jabin,^b L. Leherte,^{*c} O. Reinaud^{*a}

Synthetic procedure and characterization of [Zn(H ₂ O)L](ClO ₄) ₂	1
Determination of the relative affinity $K_{\text{MeCN}/\text{H}_2\text{O}}$ ($= K_1$).....	3
Kinetic measurements for the MeCN/EtCN guest exchange process inside the cavity of [Zn(G)L] ²⁺	5
Kinetic measurements for the MeCN/H ₂ O guest exchange process inside the cavity of [Zn(G)L] ²⁺	7
Computational details.....	10
Calixarene-MeCN interacting with a water molecule in vacuum at 300 K.....	12
Calixarene-MeCN interacting with a water molecule in acetone at 300 K and 1 bar.....	14
Calixarene-EtCN interacting with a water molecule in vacuum at 300 K.....	16
References.....	19

Synthetic procedure and characterization of [Zn(H₂O)L](ClO₄)₂



L (17.5 mg, 1 eq) and Zn(ClO₄)₂·6H₂O (4.9 mg, 1 eq.) were dissolved in acetone (2 mL) under Ar and heated at 50 °C overnight. The complexation was followed by ¹H NMR spectroscopy. The mixture was evaporated, the residue dissolved in CHCl₃ and filtrated through a syringe filter. The filtrate was evaporated and the solid washed with pentane (5 mL) to yield a colorless solid (20.2 mg, 95 %).

¹H NMR (500 MHz, acetone-d₆, 300 K) δ 8.49 (t, $J = 7.8$ Hz, 3H, H_{py}), 8.41 (d, $J = 7.7$ Hz, 3H, H_{py}), 7.90 (d, $J = 7.7$ Hz, 3H, H_{py}), 7.45 (s, 6H, H_{Ar}), 7.31 (s, 6H, H_{Ar}), 5.65 (s, 6H, OCH₂), 4.82 (s, 6H, NCH₂), 4.38 (d, $J = 14.6$ Hz, 6H, ArCH_{ax}), 3.49 (d, $J = 14.6$ Hz, 6H, ArCH_{eq}), 3.12 (s, 9H, OMe), 1.32 (s, 27H, tBu), 1.15 (s, 27H, tBu).

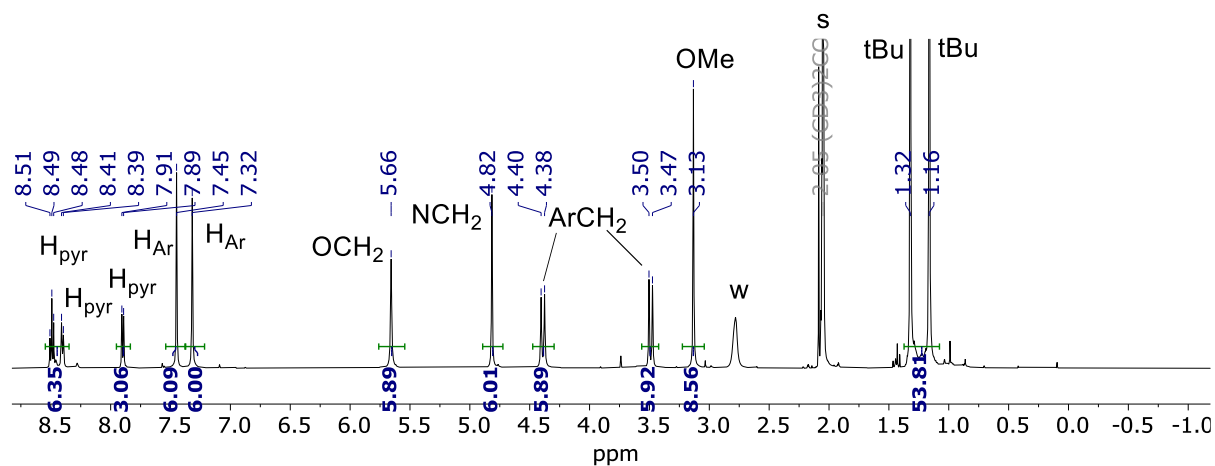


Figure S1. ¹H NMR spectrum (500 MHz, 300 K) of [Zn(H₂O)L](ClO₄)₂ in acetone-d₆.

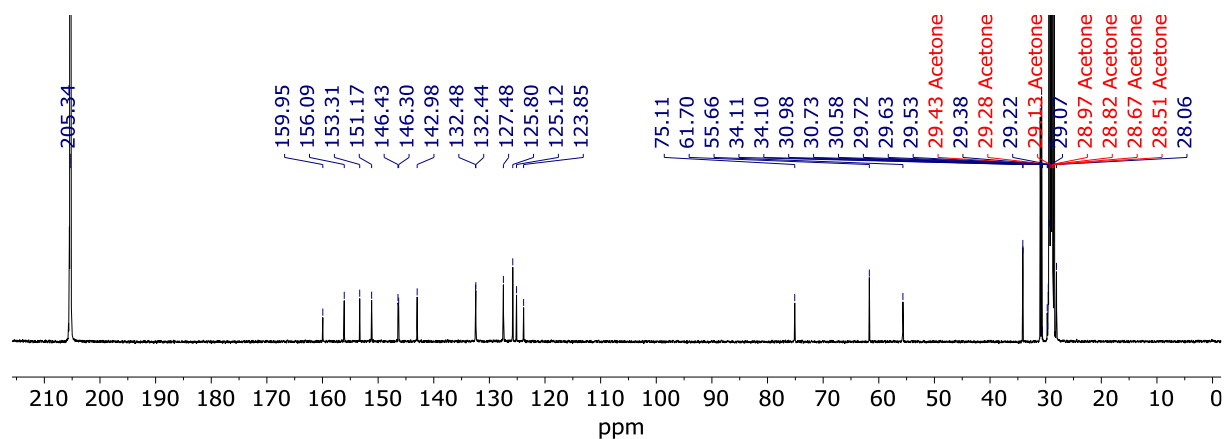


Figure S2. ¹³C NMR spectrum (126 MHz, 300 K) of [Zn(H₂O)L](ClO₄)₂ in acetone-d₆.

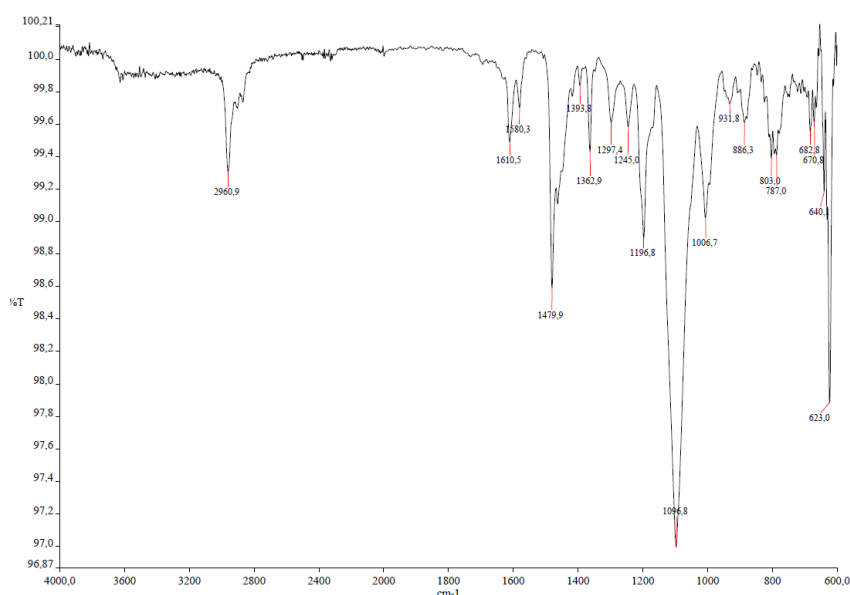


Figure S3. IR spectrum of [Zn^{II}(H₂O)L](ClO₄)₂ (solid deposition). The relative integration of the 1363 cm⁻¹ (characteristic of the calixarene core) and 623 cm⁻¹ (ClO₄⁻) bands reveals the presence of 2 ClO₄⁻.

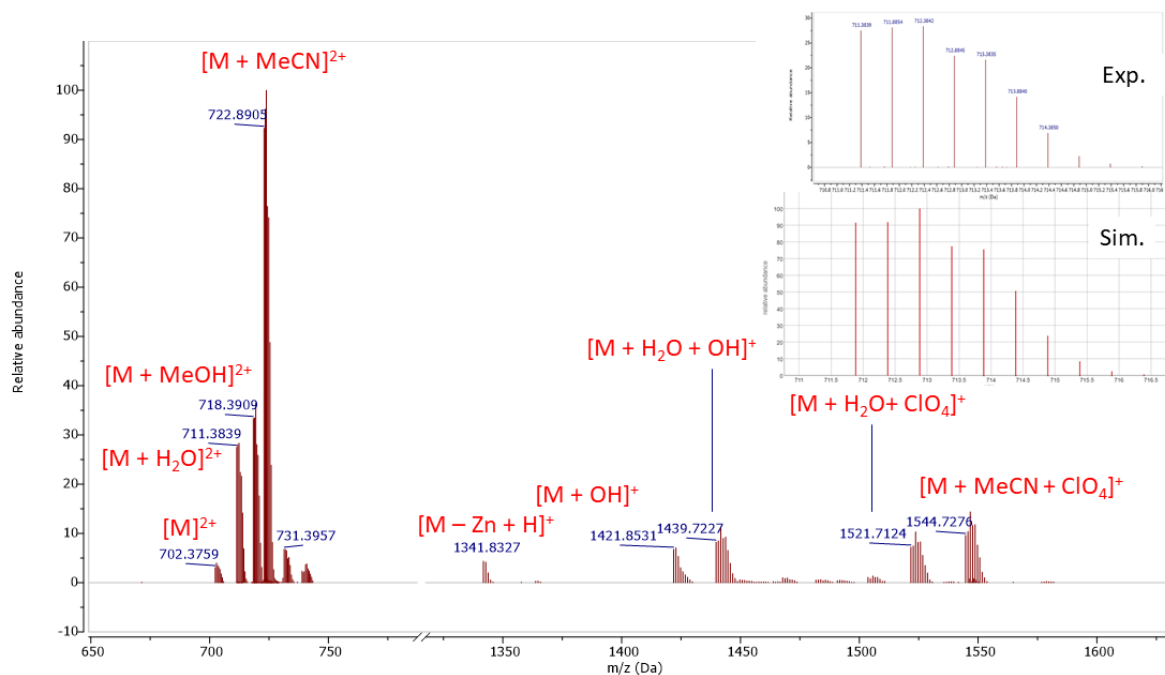


Figure S4. ESI-HRMS of $[\text{Zn}(\text{H}_2\text{O})\text{L}](\text{ClO}_4)_2$ (in acetone): m/z ($M = [\text{Zn L}] = \text{C}_{90}\text{H}_{108}\text{ZnN}_4\text{O}_6 = \text{calc. } 1404.75602$): 711.38392 ($[\text{M}+\text{H}_2\text{O}]^{2+}$ calc. 711.38275), 1421.75822 ($[\text{M}-\text{H}+\text{H}_2\text{O}]^+$ calc. 1421.85307), 1439.7227 ($[\text{M}-\text{H}+2\text{H}_2\text{O}]^+$ calc. 1439.7688), 1521.71242 ($[\text{M}+\text{H}_2\text{O}+\text{ClO}_4]^+$ calc. 1521.71456). Inset: Experimental and simulated isotopic profile of $[\text{M}+\text{H}_2\text{O}]^{2+}$.

Note: the presence of the MeCN complex stems from traces of MeCN inevitably present in the mass spectrometer, even after long washing, and is due to the very high affinity of MeCN for metal complexes based on ligand **L**.

Determination of the relative affinity $K_{\text{MeCN}/\text{H}_2\text{O}} (= K_1)$



$$\text{With: } K_1 = K_{\text{MeCN}/\text{H}_2\text{O}} = \frac{[\text{Zn}(\text{MeCN})\text{L}]^{2+} \times [\text{H}_2\text{O}]^n}{[\text{MeCN}] \times [\text{Zn}(\text{H}_2\text{O})\text{L}]^{2+}}$$

A solution of complex $[\text{Zn}(\text{MeCN})\text{L}](\text{ClO}_4)_2$ in acetone- d_6 was titrated with aliquots of water. The relative amount of each species present in solution was determined by integration of several peaks characteristic of these species, knowing the absolute amount of MeCN added to the solution.

By plotting $\{[\text{MeCN}] \times [\text{Zn}(\text{H}_2\text{O})\text{L}]^{2+}\}$ as a function of $\{[\text{Zn}(\text{MeCN})\text{L}]^{2+} \times [\text{H}_2\text{O}]^n\}$ at different concentrations of water, the linearity is obtained for $n = 1$ whereas for $n = 2$ no fit is obtained (*vide infra*). This shows an exchange process involving only one molecule of water and the corresponding $K_{\text{MeCN}/\text{H}_2\text{O}} = 200 \pm 12$. This value also highlights the higher affinity of the complex for MeCN compared to water.

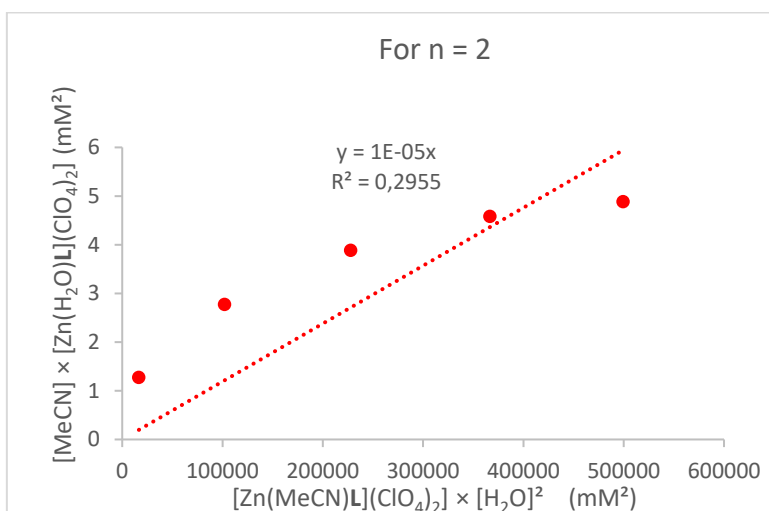
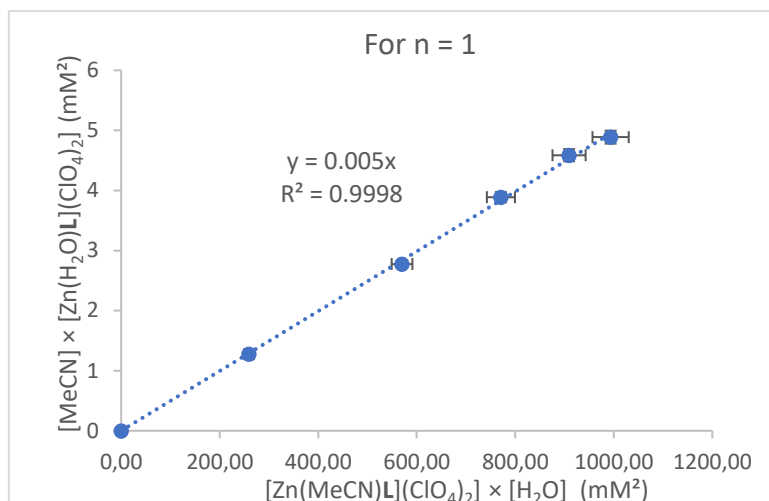


Figure S5. Determination of K_1 at different concentrations of water for $n = 1$ (Top) or $n = 2$ (Bottom).

Kinetic measurements for the MeCN/EtCN guest exchange process inside the cavity of $[Zn(G)L]^{2+}$

The concentration of initial Zn complex is obtained by preparing a stock solution of the complex by weighting the mass of the solid and then the mass of the acetone d-6 in which it is solubilized. A portion of that solution is taken (usually around 500-600 μ L) and put into a pre-weighted NMR tube. The exact volume of liquid into the NMR tube is obtained by weighting the filled NMR tube. The concentrations of water, bound and free EtCN are obtained by integration of the signals and compared to the integration of total Zn complex in solution. The concentration of MeCN is calculated from the known amount of MeCN stock solution added to the NMR tube. A typical guest exchange experiment is shown in Fig. S6

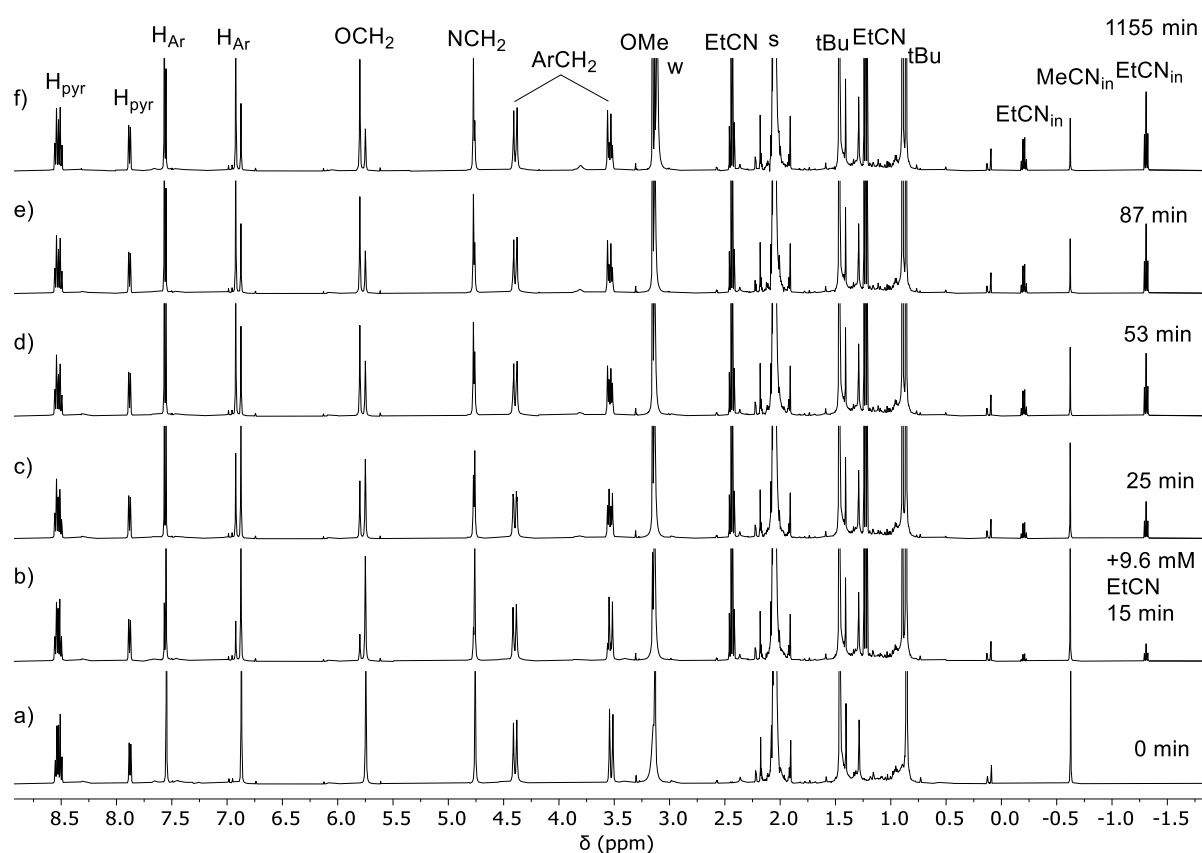


Figure S6. ^1H NMR spectra (300 K, 500 MHz, acetone- d_6) recorded during the titration of $G = \text{MeCN}$ by $G' = \text{EtCN}$. Initial conditions in a) $[\text{Zn}(\text{MeCN})\text{L}] = 3.7 \text{ mM}$, $[\text{Free MeCN}] = 92 \text{ mM}$, $[\text{EtCN}] = 0 \text{ mM}$, $[\text{H}_2\text{O}] = 20 \text{ mM}$. Percentage of propionitrile complex in solution. a) 0%, b) 17%, c) 38%, d) 41%, e) 59%, f) 71%. This experiment is reported as entry A in Table 1. Full conversion corresponds to the maximum amount of EtCN complex formed in the experiments conditions without further addition of EtCN. In this case, full conversion = spectrum f) at 71%. The “50% conversion” is then the time where we have 35.5% of EtCN complex in solution.

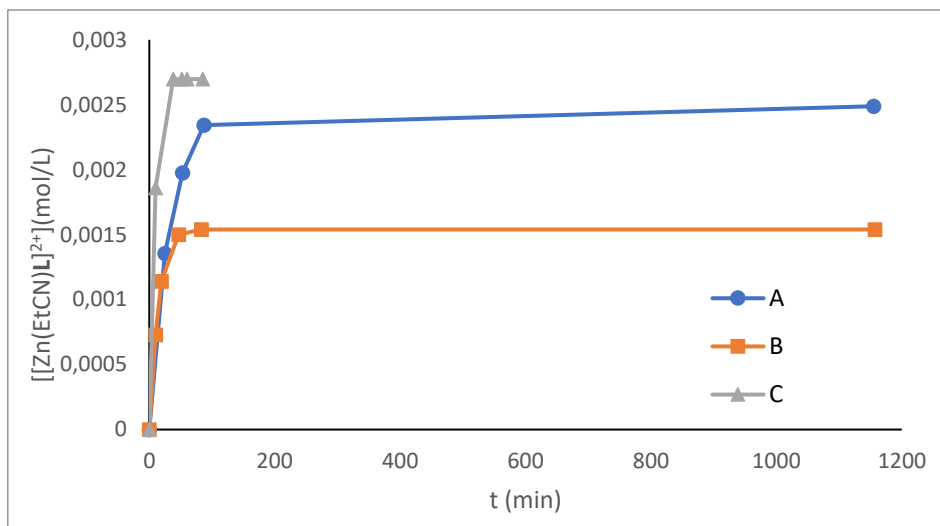


Figure S7. Evolution of $[\text{Zn}(\text{EtCN})\text{L}]^{2+}$ over time. A, B and C correspond to the experiments reported in Table 1 of the main text.

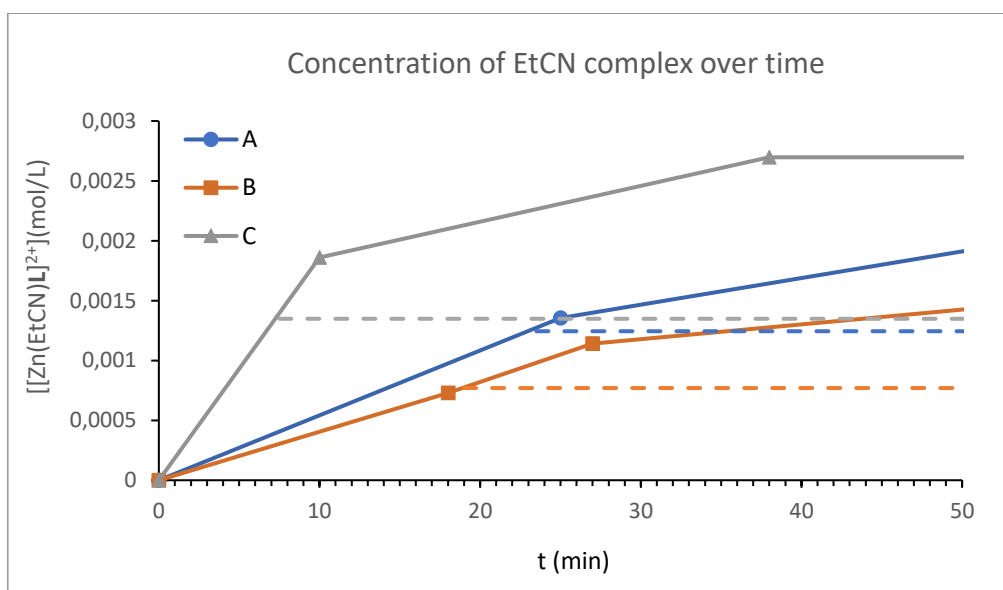


Figure S8. Zoom of Figure S7: Determination of the 50% conversion value. Full conversion corresponds to the maximum amount of EtCN complex formed in the experiments conditions without further addition of EtCN (the plateau reached in all 3 experiments).

Kinetic measurements for the MeCN/H₂O guest exchange process inside the cavity of [Zn(G)L]²⁺

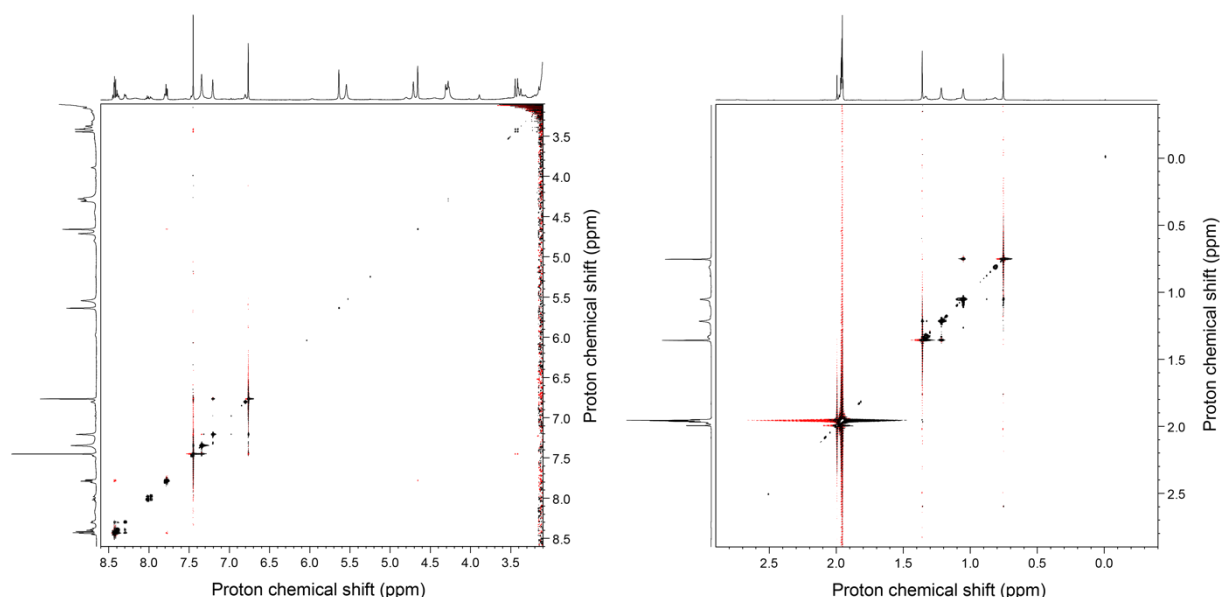


Figure S9. Selected regions of the 2D ¹H-¹H NOESY/EXSY spectrum shown in Figure 4, recorded on a solution containing a mixture of the aqua and MeCN Zn complex [Zn(H₂O)L](ClO₄)₂ in acetone-d₆. This experiment was acquired on a Bruker Avance III NMR spectrometer operating at a proton resonance frequency of 500 MHz, equipped with a dual ¹H/¹³C cryogenically cooled probehead. The standard NOESY pulse sequence was used. For each of the 1024 increments in the indirect time domain, a free induction decay of 4096 points was acquired, with 4 scans and a 3s recycle delay between scans. The mixing time was set to 1500 ms. Non uniform sampling acquisition mode was used, with an amount of sparse sampling of 50% to accelerate the acquisition. The spectral window was set to 9.7 ppm in both dimensions. Data were processed by using zero-filling up to 2048 points in the indirect dimension, and 8192 points in the direct one, apodization of 0.5 Hz and automatic baseline correction in both dimensions.

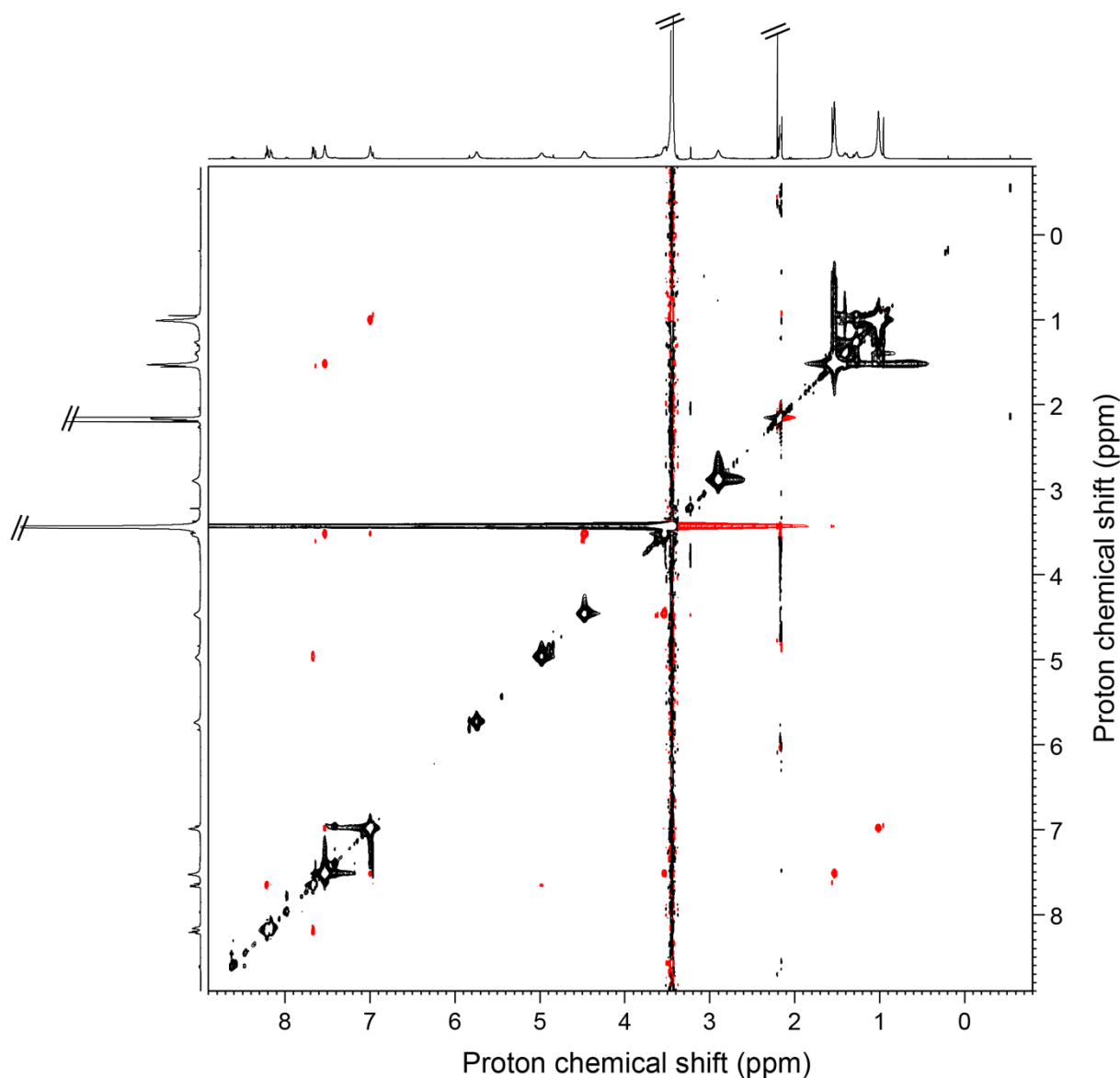


Figure S10. A representative 2D ^1H - ^1H NOESY/EXSY spectrum of a solution containing a mixture of the aqua and MeCN Zn complex $[\text{Zn}(\text{H}_2\text{O})\text{L}](\text{ClO}_4)_2$ in acetone- d_6 , recorded with a mixing time of 800 ms. This spectrum was acquired within a series of six experiments recorded with different mixing times (100, 200, 400, 800, 2000, 5000 ms), on a 600 MHz Bruker Avance IVDr spectrometer equipped with a dual $^1\text{H}/^{13}\text{C}$ probe head, to monitor the exchange processes at play in the investigated complex. This sample was prepared with 1.8 eq. of MeCN and 450 eq. of H_2O to tune the rate of the exchange process to the timescale allowed by the longitudinal relaxation times of the proton sites that were analyzed (see below). The standard NOESY pulse sequence was used. For each of the 1024 increments in the indirect time domain, a free induction decay of 4096 points was acquired, with 4 scans and a 3s recycle delay between scans. Non uniform sampling acquisition mode was used, with an amount of sparse sampling of 50% to accelerate the acquisition. The quantitativity of the resulting data was controlled in a preliminary test by comparing with the same data recorded using the traditional acquisition mode (uniform sampling of the indirect time domain). The spectral window was set to 9.7 ppm. Data were processed by using zero-filling up to 2048 points in the indirect domain, and 8192 points in the direct one, apodization of 0.5 Hz and automatic baseline correction in both dimensions.

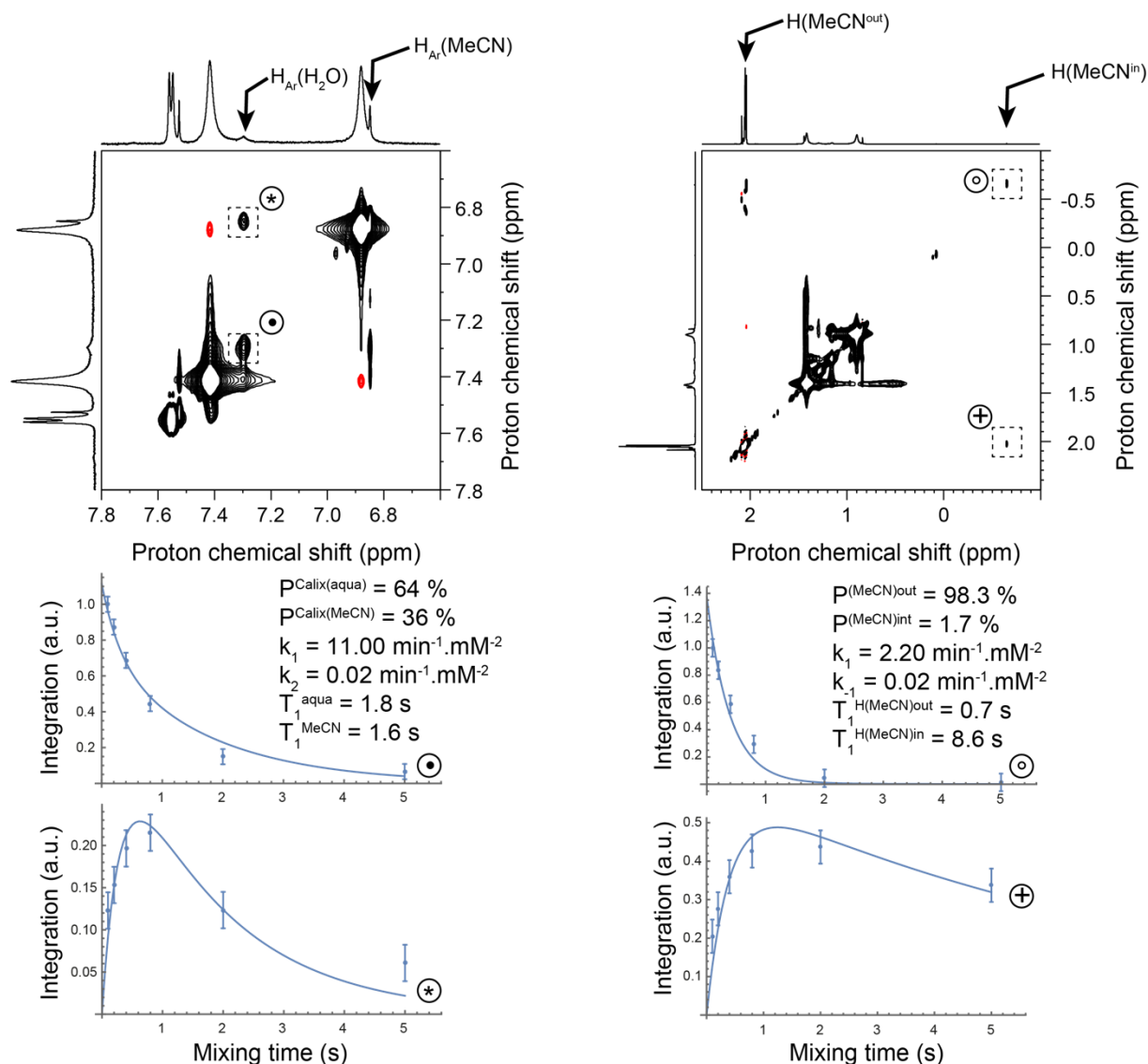


Figure S11. (Top) The regions of interest of the 2D EXSY spectrum showing the correlation patterns assigned to the proton sites that highlight the exchange process between the aqua and MeCN Zn complex (6.85 / 7.3 ppm) on the one hand, and bound and free MeCN (-0.7 / 2.0 ppm) on the other hand. (Bottom) The evolution of the correlation volumes obtained by varying the mixing time from 0.1 s to 5.0 s at 300 K. For each proton site, the evolution of the selected diagonal and cross peaks arising from the exchange process was fitted using modified Bloch equations to model the evolution of the proton longitudinal magnetization during the mixing time, under the effect of longitudinal relaxation and a standard 2-sites exchange process (cross relaxation with other proton sites was neglected). The parameters that were adjusted for each set of signals (respectively H_{Ar} from the complex, and H_{MeCN}) are the rate constants k_1 and k_{-1} (see main text), and the longitudinal relaxation time (T_1) for each proton site. The populations P of the two exchanging proton sites were estimated from the deconvolution and the integration of their respective signals measured on a 1D ^1H spectrum. The following concentration values were used to calculate k_1 and k_{-1} from the apparent rates determined during the fitting of EXSY data: $[\text{MeCN}] = 9.8 \text{ mMol} \cdot \text{L}^{-1}$, $[\text{Zn}(\text{H}_2\text{O})\text{L}]^{2+} = 0.3 \text{ mMol} \cdot \text{L}^{-1}$, $[\text{Zn}(\text{H}_2\text{O})\text{L}]^{2+} = 0.5 \text{ mMol} \cdot \text{L}^{-1}$, and $[\text{H}_2\text{O}] = 2570 \text{ mMol} \cdot \text{L}^{-1}$.

Computational details

Initial structure of the calixarene-MeCN complex

Starting from the $[\text{Cu}^{\text{II}}(\text{NCEt})\text{L}](\text{ClO}_4)_2$ crystal structure,^[1] the Cu^{II} ion was replaced by Zn^{II} . A PM7 semi-empirical optimization was carried out with the program MOPAC2016^[2] after having moved the water molecule so as to avoid any chemical bond with the acetonitrile (MeCN) guest. The default optimization algorithm and parameters were used. The resulting structure suggested a potentially stable complex with both the MeCN and H_2O placed inside the calixarene cavity. The H_2O molecule was further deleted to generate the MD input files.

To study the exchange of water and MeCN through MD simulations, MeCN and the empty calixarene structures were submitted to the Swissparam server^[3] to generate the input coordinates and topology files suitable for the GROMACS2020 MD simulations^[4]. On the whole, the complete coordinate file was built by merging the calixarene, Zn, and MeCN coordinates. Similarly, a full topology file was built to call for calixarene, Zn, and MeCN force field parameters.

To study complexes with propionitrile (EtCN) rather than acetonitrile as the guest, MeCN was replaced by EtCN in the calixarene complex optimized with MOPAC2016. The EtCN structure was retrieved from the free Chemical Entities of Biological Interest (ChEBI) web site^[5] and its coordinates were obtained through a EtCN-MeCN superimposition procedure of the C-C \equiv N moiety. The EtCN topology file that is suitable for GROMACS MD simulations was also obtained using the server Swissparam.^[3] A MeOH topology file was also obtained using the same approach.

MD and SMD simulations of the guest substitution

All MD simulations were carried out with the software GROMACS2020 at 300 K, either in vacuum or in acetone (at 1 bar). In that last case, the initial calixarene-MeCN structure was solvated in acetone whose liquid box coordinates were retrieved from the compound database of the Virtual Chemistry web site.^[6] The initial system size has dimensions of 6.773 x 4.773 x 4.773 nm. Two chloride ions were added to neutralize the system which contains 1184 acetone molecules.

To further allow SMD calculations which require the application of a pulling force on the guest, the initial guest/calixarene structure was oriented along the x-axis of the Cartesian coordinate system.

To avoid too strong a deformation of the calixarene during the MD simulations, distance restraints were applied between the Zn^{II} ion and the four N atoms of the calixarene cap, with lower and upper cut-off values of 0.20 and 0.22-0.23 nm, and a large force constant value of 50,000 $\text{kJ mol}^{-1} \text{nm}^{-2}$. Also, to prevent the calixarene structure from accompanying the guest displacement during the pulling stage, the N atoms of the calixarene cap were held in place using a force constant of 5,000 $\text{kJ mol}^{-1} \text{nm}^{-2}$ in each direction.

The complete systems were optimized to eliminate large forces using a Steepest Descent procedure with a tolerance of $1.0 \text{ kJ mol}^{-1} \text{ nm}^{-1}$ and an initial step size of 0.05 nm . A maximum number of 5,000 iterations was allowed.

The systems were then heated to 50 K through a 10 ps NVT MD, with a time step of 2 fs and LINCS constraints acting on bonds involving H atoms. The trajectory was followed by two successive 20 ps heating stages, at 150 and 300 K under the same conditions. Next, each system was equilibrated during $2,050 \text{ ps}$ in the NVT ensemble in vacuum, and in the NPT ensemble in a solvent, using the thermostat V-rescale and barostat Berendsen algorithms. Snapshots were saved every 50 iterations. Altogether, the MD and SMD calculations build a trajectory of $2,160 \text{ ps}$ ($21,601$ snapshots or frames).

During all MD simulations, the vdW cut-off distance was set equal to 1.2 nm with a force switch set at 1.0 nm . In vacuum, the Coulomb cut-off parameter was set equal to 1.2 nm as well. In solution, a Particle Mesh Ewald (PME) Periodic Boundary Conditions (PBC) scheme was applied to calculate the long-range electrostatic interactions with a cut-off of 1.2 nm too.

The SMD procedure was applied to the last frame of the equilibration stage. It consisted in applying a pulling force to the guest center-of-mass, along the x-axis, while restraining the N atoms of the calixarene cap at their optimized position. The SMD pulling stage was carried out for 30,000 iterations, with a time step of 2 fs , a harmonic “umbrella” force constant of $1,000 \text{ kJ mol}^{-1} \text{ nm}^{-2}$, and a pulling rate of 0.025 nm ps^{-1} .

Calixarene-MeCN interacting with a water molecule in vacuum at 300 K

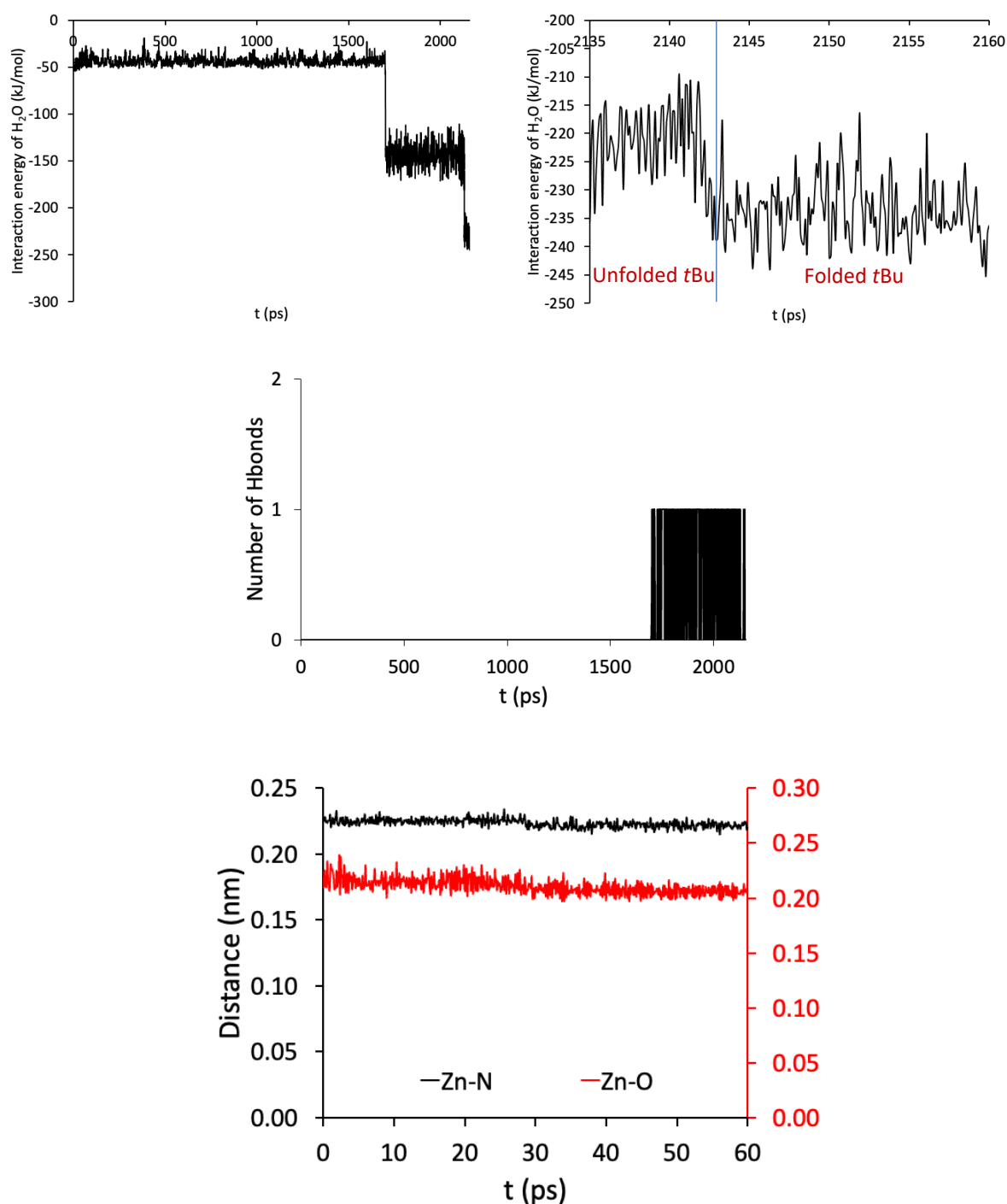


Figure S12. Profiles obtained from the 2,160 ps long simulation of the calixarene-MeCN system interacting with a water molecule, in vacuum at 300 K. (Top Left) Intermolecular interaction energy profile of the water molecule with the calixarene-MeCN complex. (Top Right) Zoom on the interaction energy of water before and after tBu folding during the final steps of the SMD simulation. (Center) Number of water-methoxy hydrogen bonds. GROMACS cut-off values for the hydrogen bonds are: D-A distance = 0.3 nm and H-D-A angle = 30°. (Bottom) Zn^{II}-N_{calix} (black) and Zn^{II}-O_{water} (red) distance profiles during the 60 ps Ion SMD trajectory.

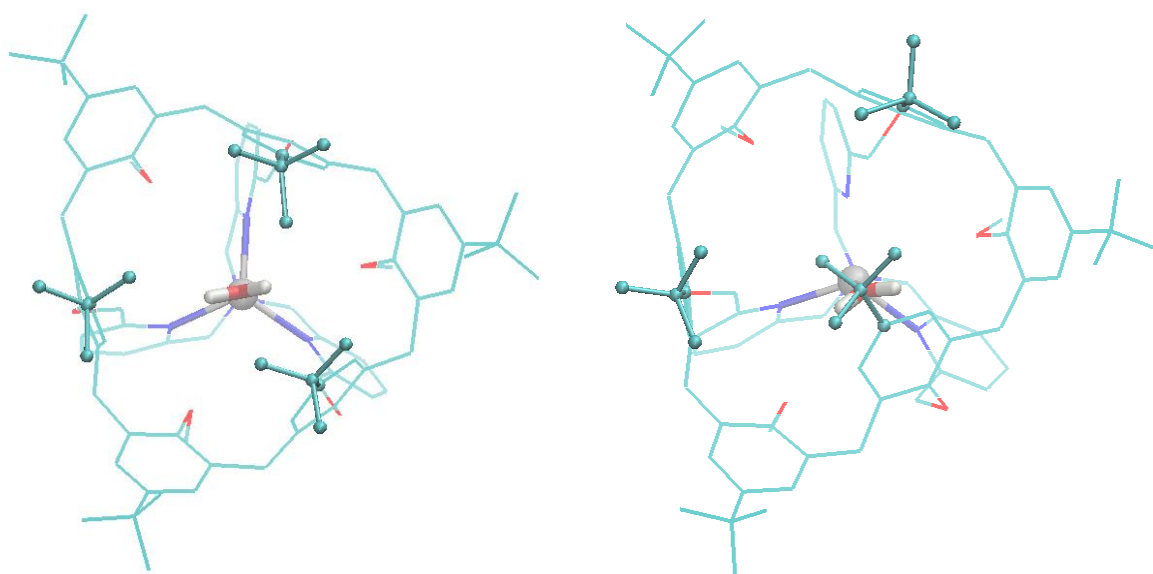


Figure S13. (Left) Snapshot at $t = 42.0$ ps and (Right) final snapshot, obtained from the 60 ps SMD simulation of the calixarene-MeCN system interacting with a water molecule, in vacuum at 300 K. (bottom views). H atoms are not shown for clarity.

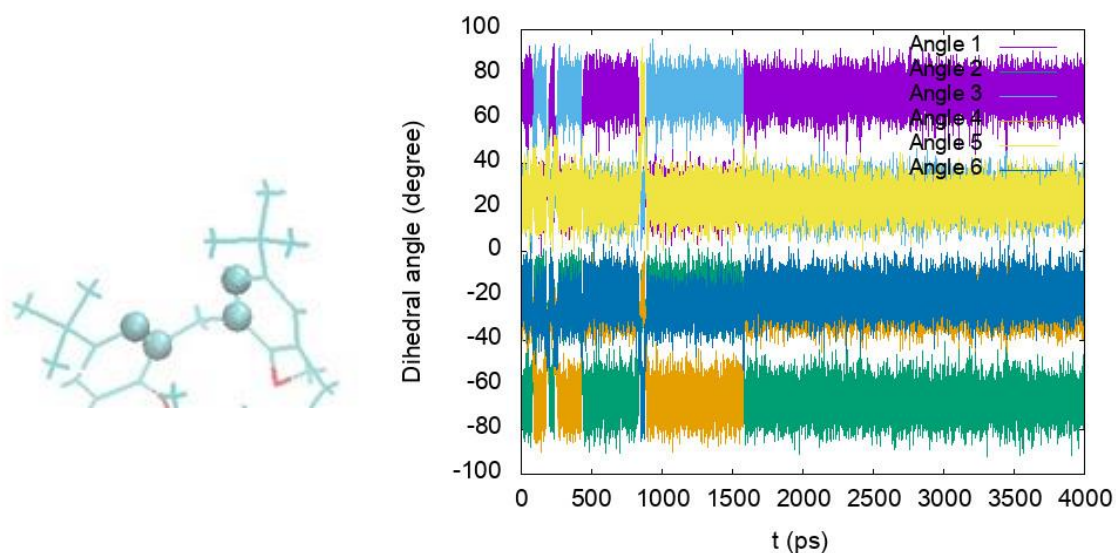


Figure S14. (Left) Atoms used to define a dihedral angle to check the *t*Bu folding during a post SMD simulation. (Right) The six dihedral angle profiles obtained from a post SMD simulation of 4,000 ps, starting from the final SMD atomic coordinates of the calixarene-H₂O system, in vacuum at 300 K.

Calixarene-MeCN interacting with a water molecule in acetone at 300 K and 1 bar

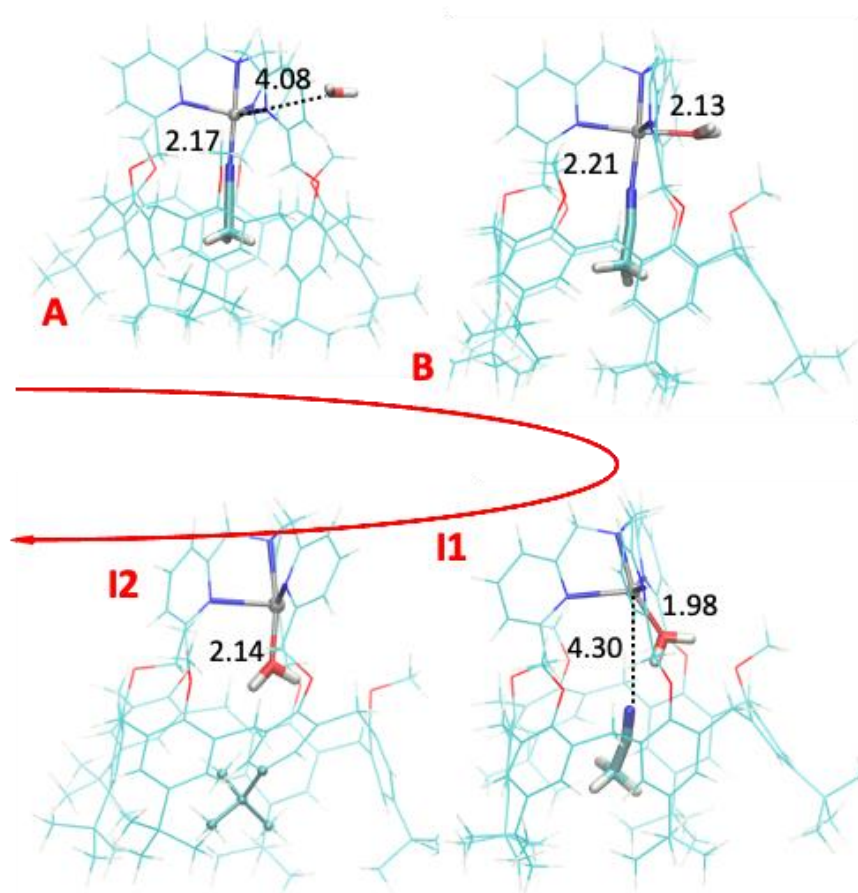


Figure S15. Stepwise substitution of the MeCN guest by a water molecule following an associative pathway, as obtained from the 2,160 ps MD and SMD trajectory in acetone at 300 K and 1 bar. Snapshots at 0 (initial optimized structure - **A**), 870.1 (coordination of H₂O - **B**), 2,109.2 (insertion stage - **I1**), 2,160.0 ps (last snapshot - **I2**). Interaction energy values of the water molecules with the calixarene complex and with the solvent are (-27.44; -31.39), (-106.85; -56.10), (-175.02; -1.45), and (-172.01; -0.61) kJ mol⁻¹, respectively. Distances are in Å. The folded *t*Bu moiety is displayed using ball and stick representations in **I2**.

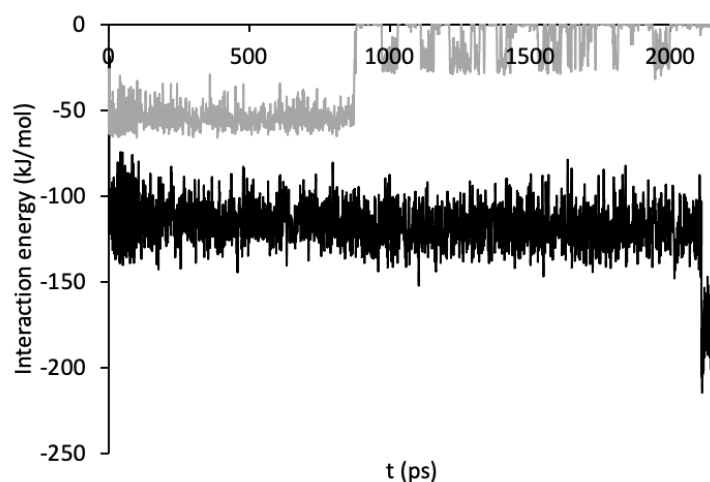


Figure S16. Short-range intermolecular interaction energy profile of the water molecule with the calixarene-acetonitrile complex (black) and with the solvent molecules (gray) as obtained from the 2,160 ps long simulation in acetone, at 300 K and 1 bar.

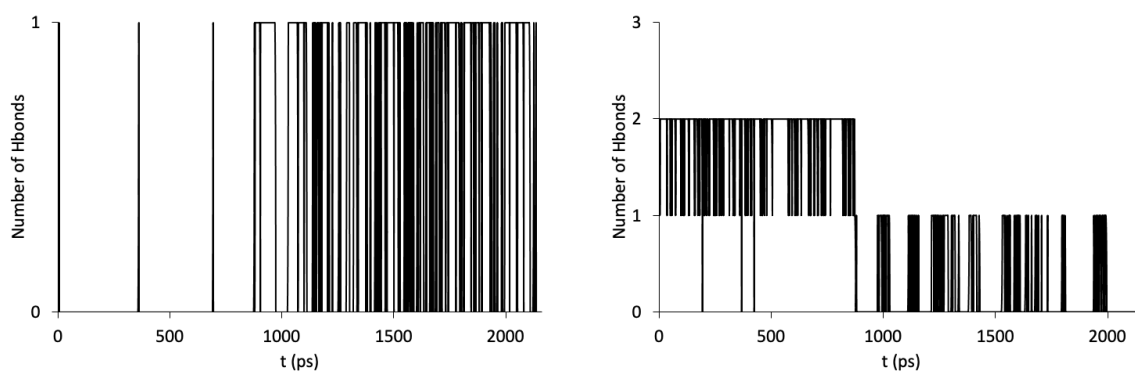


Figure S17. Number of hydrogen bonds occurring between the water molecule and (Left) the calixarene O_{methoxy} atoms, (Right) the acetone molecules, as obtained from the 2,160 ps simulation in acetone, at 300 K and 1 bar. GROMACS cut-off values for the hydrogen bonds are: D-A distance = 0.3 nm and H-D-A angle = 30° .

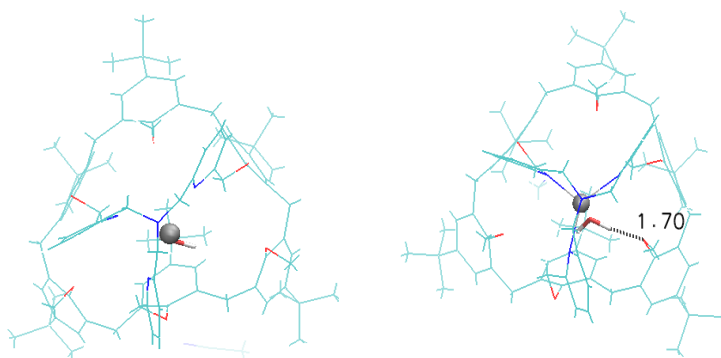


Figure S18. (Left) Final snapshot obtained from the 60 ps SMD simulation of the calixarene-water system in acetone, at 300 K and 1 bar and (Right) its optimized version using MOPAC2016 (top views). Distance in Å.

Calixarene-EtCN interacting with a water molecule in vacuum at 300 K

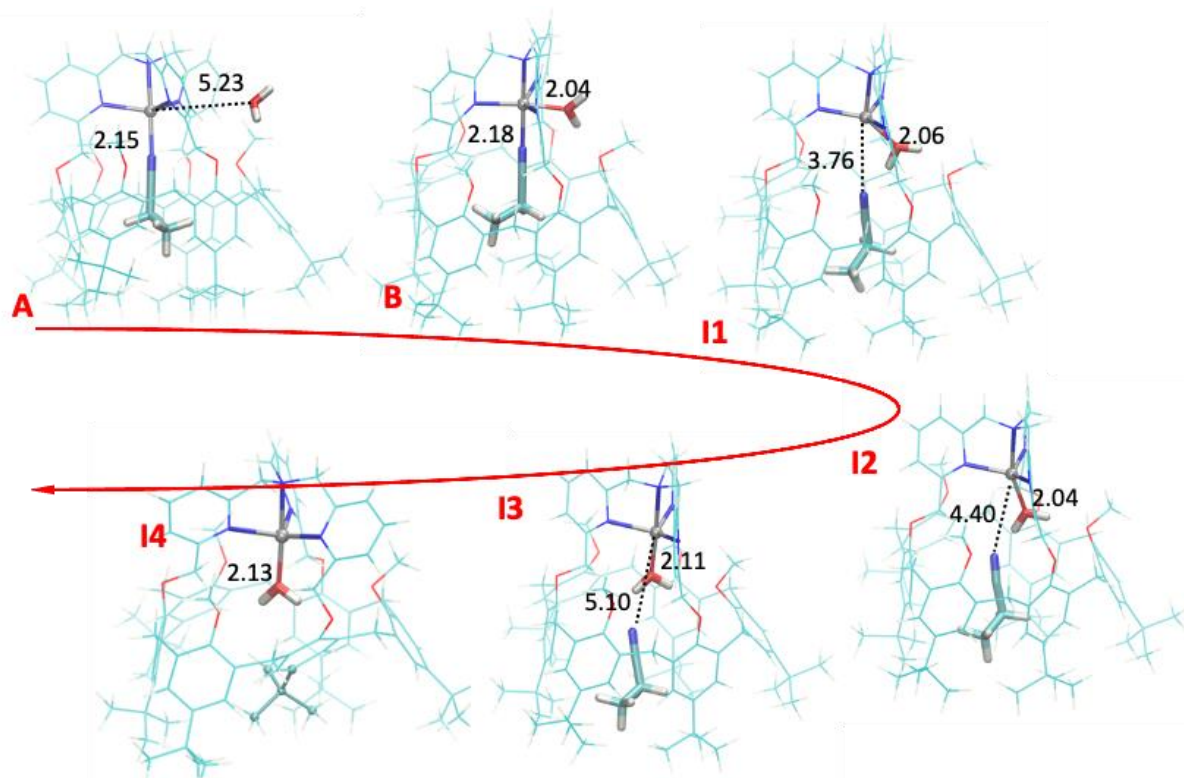


Figure S19. Stepwise substitution of the EtCN guest by a water molecule following an associative pathway, as obtained from the 2,160 ps MD and SMD trajectories in vacuum at 300 K. Snapshots at 0 (optimized structure - **A**), 353.9 (coordination of H₂O - **B**), 2,132.1 (insertion stage - **I1**), 2,132.2 (insertion stage - **I2**), 2,132.3 (insertion stage - **I3**), and 2,160.0 ps (final structure - **I4**). Interaction energy values of the water molecules are -38.71, -117.86, -170.25, -235.63, -235.51, and -236.94 kJ mol⁻¹, respectively. Distances are in Å. The folded *t*Bu moiety is displayed using ball and stick representations in **I4**.

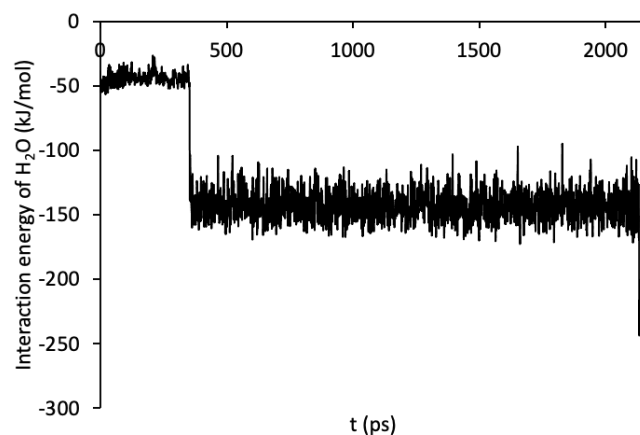


Figure S20. Intermolecular interaction energy profile of the water molecule with the calixarene-EtCN complex as obtained from the 2,160 ps simulation in vacuum, at 300 K.

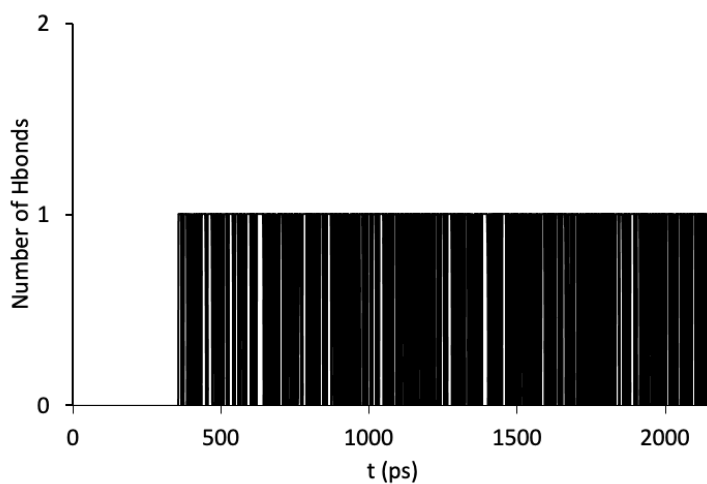


Figure S21. Number of hydrogen bonds occurring between the water molecule and a methoxy group of the calixarene structure as obtained from the 2,160 ps simulation in vacuum, at 300 K. GROMACS cut-off values for the hydrogen bonds are: D-A distance = 0.3 nm and H-D-A angle = 30° .

A hydrogen bond is formed at 354 ps, well before the H bond formation time observed during the MD simulation of the calixarene-MeCN-water case (cf. SI). It has no physical significance since a different starting MD state may have led to a different occurrence time of the H bond.

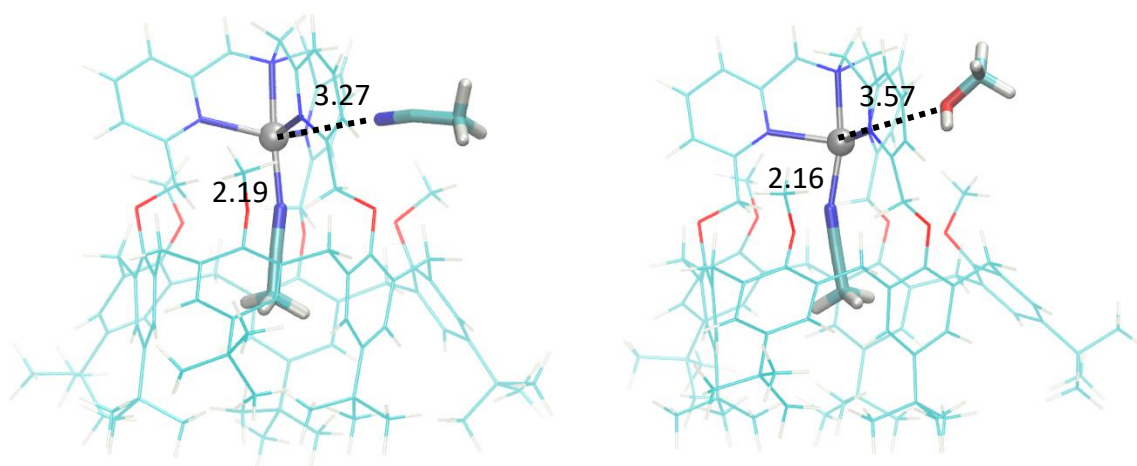


Figure S22. Snapshots obtained from the 2,100 ps long MD simulations of the calixarene-MeCN system in vacuum, at 300 K. The *exo*-ligand is (Left) MeCN at $t = 613.5$ ps, (Right) MeOH at $t = 771.7$ ps. Distances are in Å.

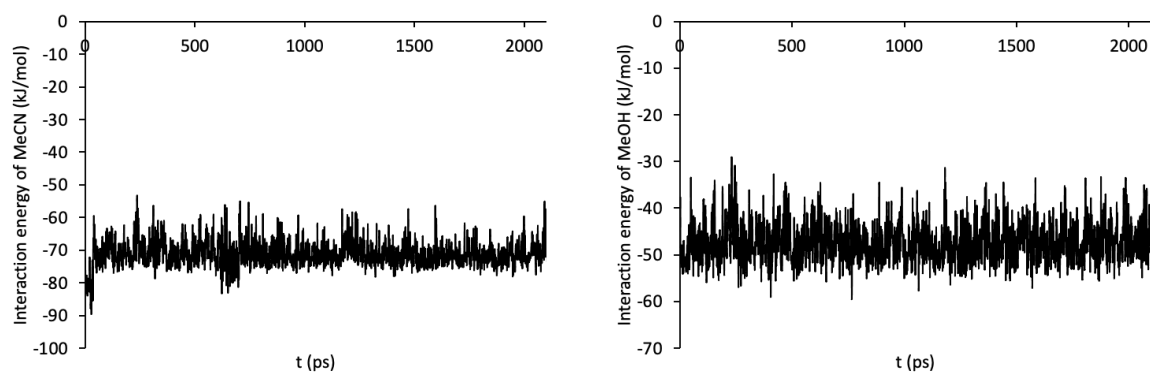


Figure S23. Intermolecular interaction energy profile of the *exo*-ligand molecule with the calixarene-MeCN complex as obtained from the 2,100 ps MD simulation in vacuum, at 300 K. The *exo*-ligand is (Left) MeCN, (Right) MeOH.

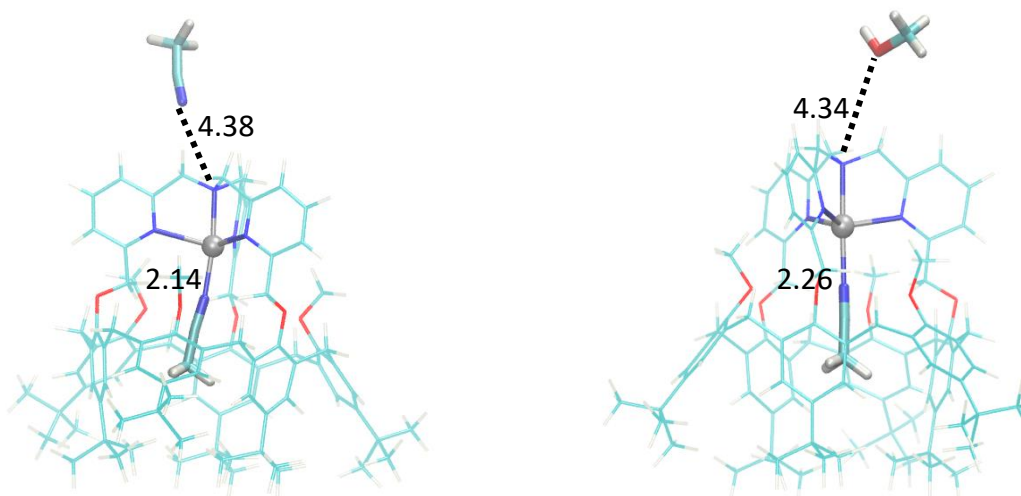


Figure S24. Last frame of the 2,100 ps long MD simulations of the calixarene-MeCN system, in vacuum at 300 K. The *exo*-ligand is (Left) MeCN, (Right) MeOH.

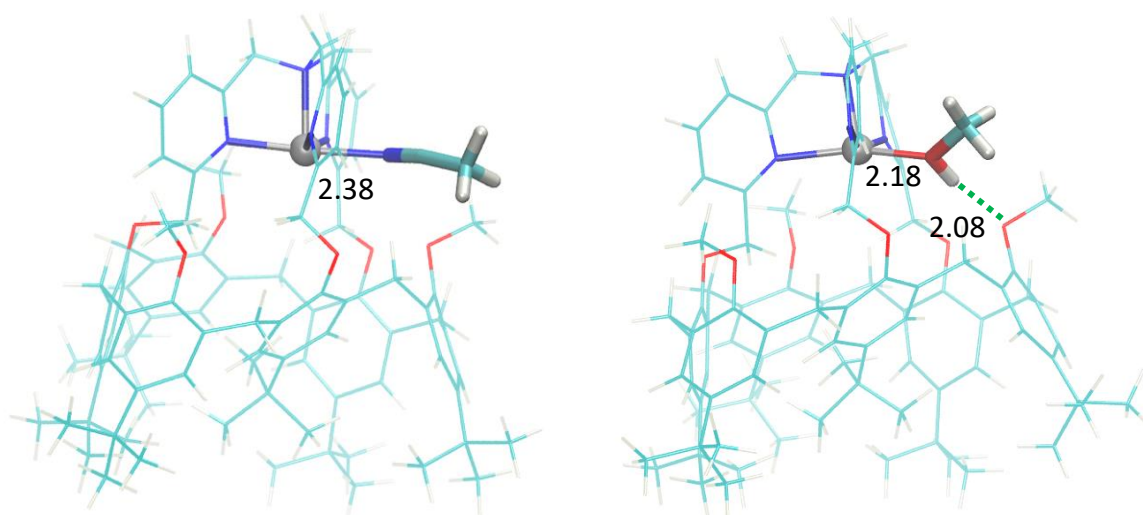


Figure S25. Last frames of the 2,100 ps long MD simulations of calixarene without *endo*-ligand, in vacuum at 300 K. The *exo*-ligand is (Left) MeCN, (Right) MeOH. H bond is displayed with green dotted line.

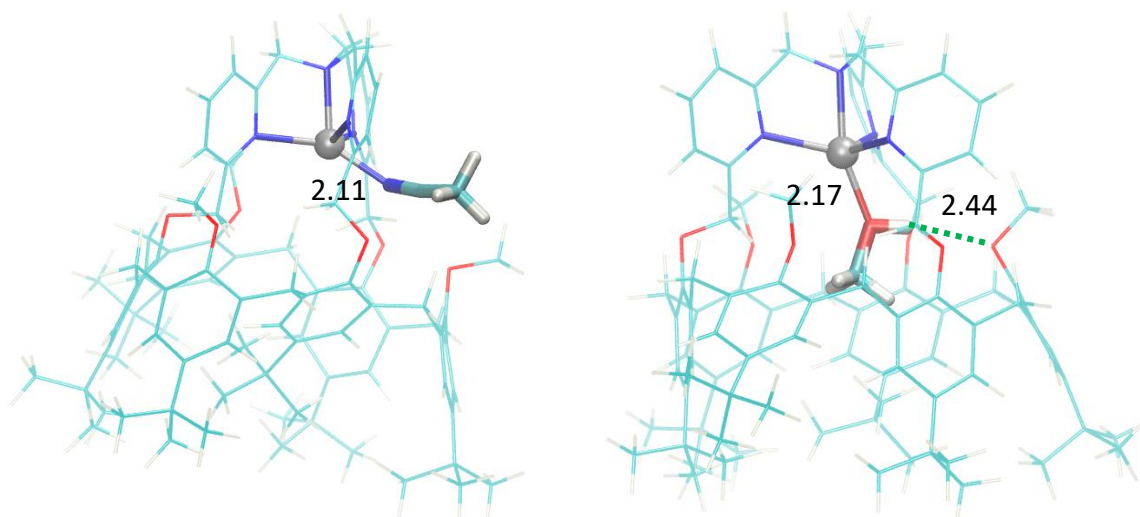


Figure S26. Snapshots obtained from the 60 ps long SMD simulations of calixarene without *endo*-ligand, in vacuum at 300 K. The *exo* ligand is (Left) MeCN at $t = 60$ ps, (Right) MeOH at $t = 41.9$ ps. Distances are in Å. H bond is displayed with green dotted line.

References

- [1] G. Izzet, X. Zeng, H. Akdas, J. Marrot, O. Reinaud, *Chem. Commun.* **2007**, 810–812.
- [2] J. J. P. Stewart, Stewart Computational Chemistry, Colorado Springs, CO, USA (2016), <http://OpenMOPAC.net> (last accessed 20 Dec. 2022).
- [3] V. Zoete, M. A. Cuendet, A. Grosdidier, O. Michielin, *J. Comput. Chem.* **2011**, *32*, 2359–2368.
- [4] M. J. Abraham, T. Murtola, R. Schulz, S. Páll, J. C. Smith, B. Hess, E. Lindahl, *SoftwareX* **2015**, *1–2*, 19–25.
- [5] J. Hastings, G. Owen, A. Dekker, M. Ennis, N. Kale, V. Muthukrishnan, S. Turner, N. Swainston, P. Mendes, C. Steinbeck, *Nucleic Acids Res.* **2016**, *44*, D1214–D1219. Data available at <https://www.ebi.ac.uk/chebi/> (last accessed 20 Dec. 2022)
- [6] D. van der Spoel, P. J. van Maaren, C. Caleman, *Bioinform. Oxf. Engl.* **2012**, *28*, 752–753. available at <https://virtualchemistry.org/molddb.php> (last accessed 20 Dec. 2022)